ORIGINAL RESEARCH

NCK Associated Protein 1 Modulated by miRNA-214 Determines Vascular Smooth Muscle Cell Migration, Proliferation, and Neointima Hyperplasia

Tayyab Adeel Afzal, Msc;* Le Anh Luong, PhD;* Dan Chen, MD; Cheng Zhang, MD; Feng Yang, MD; Qishan Chen, MD, PhD; Weiwei An, PhD; Edmund Wilkes, PhD; Kenta Yashiro, MD, PhD;† Pedro R. Cutillas, PhD; Li Zhang, MD, PhD; Qingzhong Xiao, MD, PhD

***Background*—**MicroRNA miR-214 has been implicated in many biological cellular functions, but the impact of miR-214 and its target genes on vascular smooth muscle cell (VSMC) proliferation, migration, and neointima smooth muscle cell hyperplasia is unknown.

***Methods and Results*—**Expression of miR-214 was closely regulated by different pathogenic stimuli in VSMCs through a transcriptional mechanism and decreased in response to vascular injury. Overexpression of miR-214 in serum-starved VSMCs significantly decreased VSMC proliferation and migration, whereas knockdown of miR-214 dramatically increased VSMC proliferation and migration. Gene and protein biochemical assays, including proteomic analyses, showed that NCK associated protein 1 (NCKAP1)—a major component of the WAVE complex that regulates lamellipodia formation and cell motility—was negatively regulated by miR-214 in VSMCs. Luciferase assays showed that miR-214 substantially repressed wild-type but not the miR-214 binding site mutated version of NCKAP1 3′ untranslated region luciferase activity in VSMCs. This result confirmed that NCKAP1 is the functional target of miR-214 in VSMCs. NCKAP1 knockdown in VSMCs recapitulates the inhibitory effects of miR-214 overexpression on actin polymerization, cell migration, and proliferation. Data from cotransfection experiments also revealed that inhibition of NCKAP1 is required for miR-214–mediated lamellipodia formation, cell motility, and growth. Importantly, locally enforced expression of miR-214 in the injured vessels significantly reduced NCKAP1 expression levels, inhibited VSMC proliferation, and prevented neointima smooth muscle cell hyperplasia after injury.

***Conclusions*—**We uncovered an important role of miR-214 and its target gene NCKAP1 in modulating VSMC functions and neointima hyperplasia. Our findings suggest that miR-214 represents a potential therapeutic target for vascular diseases. **(*J Am Heart Assoc*. 2016;5:e004629 doi: 10.1161/JAHA.116.004629)**

Key Words: cell migration • cell proliferation • microRNA • miRNA-214 • NCK-associated protein 1 • neointimal hyperplasia • vascular biology • vascular disease • vascular smooth muscle

Vascular smooth muscle cells (VSMCs) are the major cellular component of the blood vessels and perform versatile functions (eg, maintaining vascular tone and regulating blood volume and pressure in the circulatory system) under normal physiological conditions. They have a profound dual role (propagating and protective) in the

From the Centre for Clinical Pharmacology, William Harvey Research Institute (T.A.A., L.A.L., D.C., C.Z., F.Y., Q.C., W.A., Q.X.), Translational Medicine & Therapeutics, William Harvey Research Institute (K.Y.), and Centre for Haemato-Oncology, Barts Cancer Institute (E.W., P.R.C.), Barts and The London School of Medicine and Dentistry, Queen Mary University of London, United Kingdom; Department of Cardiothoracic Surgery, The First Affiliated Hospital of Chongqing Medical University, Chongqing, China (D.C., C.Z.); Department of Cardiology, The First Affiliated Hospital, School of Medicine, Zhejiang University, Hangzhou, Zhejiang, China (F.Y., Q.C., L.Z.).

Accompanying Figures S1, S2 and Tables S1 through S3 are available at http://jaha.ahajournals.org/content/5/12/e004629/DC1/embed/inline-supplementary-material-1.pdf

*Dr Afzal and Dr Luong contributed equally to this study.

†Dr Kenta Yashiro is currently located at Department of Cardiovascular Surgery, Cardiac Regeneration and Therapeutics, Osaka University Graduate School of Medicine, Yamada-oka 2-2, Suita, Osaka 565-0871, Japan.

Correspondence to: Qingzhong Xiao, MD, PhD, Centre for Clinical Pharmacology, William Harvey Research Institute, Barts and The London School of Medicine and Dentistry, Queen Mary University of London, Heart Centre, Charterhouse Square, London EC1M 6BQ, United Kingdom. E-mail: q.xiao@qmul.ac.uk or Li Zhang, MD, PhD, Department of Cardiology, the First Affiliated Hospital, School of Medicine, Zhejiang University, 79 Qingchun Road, Hangzhou, 310003 Zhejiang, China. E-mail: li.zhang.uk@googlemail.com

Received September 8, 2016; accepted October 28, 2016.

development and progression of atherosclerotic lesions. It has been widely known that VSMC proliferation and migration facilitate early lesion development but are equally important for maintaining plaque stability through the maintenance of a protective fibrous cap overlying the thrombotic lipid core of advanced lesions.[1] Consequently, investigating key regulators and signaling pathways governing VSMC proliferation and migration within different developmental stages of atherosclerotic lesions will facilitate and inform future strategies to modulate the disease process.

MicroRNAs (miRNAs) are endogenous, highly conserved, single-strand, short (20–23 nucleotides), noncoding RNAs. They regulate target gene expression at the posttranscription level by interacting with the 3′ untranslated regions (3′UTRs) of the specific mRNAs.[2] The fact that a single miRNA can target and regulate multiple mRNAs, and single mRNA can be targeted and regulated by multiple miRNAs makes miRNAs stand out as the key gene regulators; they control many fundamental biological processes including cell proliferation, migration, differentiation, apoptosis, senescence, and aging.[3] Unsurprisingly, miRNAs have been extensively implicated in various human diseases.[4] A handful miRNAs, including miR-1,[5] miR-21,[6,7] miR-34a,[8] miR-133,[9] miR-221/222,[10,11] the miR-143/145 cluster,[12–15] miR-638,[16] and miR-663,[17] have been recently reported to play roles in modulating the processes of vascular diseases by regulating various VSMC functions; however, the significance and regulatory roles of other miRNAs in regulating VSMC functions and in the development of vascular diseases are still not fully understood.

In particular, a contradictory but pivotal role of miR-214 (protective and pathological) in cardiovascular disease and cancer has been suggested based on recent studies. miR-214 is upregulated in response to several factors including cardiac stress, myocardial infarction, and Ca^{2+} overload.[18,19] It has been reported that miR-214 protects myocardial cells against excessive Ca^{2+} uptake during ischemia–reperfusion injury by repressing mRNA-encoding sodium/calcium exchanger 1 (Ncx1), thus maintaining Ca^{2+} homeostasis and increasing cell survival.[20] In another study, a decrease in miR-214 levels was associated with an increase in placental growth factor levels and worsening of atherosclerosis, suggesting its role as a protective agent and a promising biomarker for severe coronary artery disease.[21] In contrast, antagonizing (inhibiting) miR-214 was suggested as a potential new therapeutic approach for treating cardiac hypertrophy or heart failure in another study.[22] These studies have provided evidence to suggest a role for miR-214 in cardiac hypertrophy; importantly, in our previous miRNA microarray study, we found that miR-214 is one of the most upregulated miRNAs during smooth muscle cell (SMC) differentiation from mouse embryonic stem cells.[23] Less is known about the functional involvement of miR-214 and its target gene in regulating VSMC functions and modulating neointima SMC hyperplasia. In this study, we demonstrated that miR-214 inhibits VSMC proliferation and migration, at least in part, by targeting NCK associated protein 1 (NCKAP1). Consequently, restoring expression of miR-214 in the diseased blood vessels would be a potential therapeutic approach for treatment of proliferative vascular diseases.

Materials and Methods

Materials

Antibody against NCKAP1 (goat, N-12, sc-161124) was purchased from Santa Cruz Biotechnology. The anti-NCKAP1 antibody used for paraffin-section staining was purchased from Antibodies-online GmbH. Antibodies against GAPDH (mouse), Ki-67 (rabbit), and proliferating cell nuclear antigen (PCNA; rabbit) were from Abcam. All secondary antibodies were from Dako. Other materials including Phalloidin-FITC (P5282) used in this study were purchased from Sigma-Aldrich unless specifically indicated.

VSMC Culture and Treatments

Primary murine VSMCs were isolated from mouse aorta and routinely maintained in DMEM supplemented with 10% FBS, as described in our previous study.[8,24] Human aortic SMCs were purchased from PromoCell GmbH (C-12533) and cultured in SMC growth medium 2 (C-22062; PromoCell GmbH), according to the manufacturer's instructions. VSMCs between passages 5 and 10 were used in the current study. VSMCs were treated with various atherogenic stimuli, as described in the previous studies.[9,25–28] Briefly, for platelet-derived growth factor BB (PDGF-BB; BioLegend) and serum stimulation, VSMCs were serum starved for 24 to 48 hours (0.5% FBS), followed by an incubation with 20% FBS and 10 ng/mL PDGF-BB for 3, 6, 12, 24, and 48 hours. For oxidized low-density lipoprotein component treatments, VSMCs were serum starved for 24 to 48 hours, followed by incubation with 10 μmol/L 4-hydroxynonenal and 7-ketocholesterol for 24 hours.

miRNA Mimics and Inhibitor Transfection

miRNA mimics and inhibitor transfection were conducted as described previously with some modifications.[8,23,29,30] Briefly, either miRNA mimics or inhibitors and miRNA-negative controls (25 nmol/L, final concentration) were transfected into VSMCs using TransIT-X2 transfection reagent (Geneflow Ltd), according to the manufacturer's instructions. VSMCs (1.5×10^5 per well) were seeded into 6-well plate 24 hours

prior to transfection. Before transfection, cells were washed with 1× PBS once and replenished with 1.75 mL fresh culture medium containing 5% FBS. TransIT-X2 reagent was warmed to room temperature. Next, 250 μL of serum-free DMEM was added to a sterile Eppendorf tube, and 5 μL of miR-214 mimics/inhibitor or their respective control scramble miRNA mimics/inhibitor (10 μmol/L in stock) was added and mixed using a pipette. We added 7.5 μL of TransIT-X2 reagent and mixed gently. This was left to incubate at room temperature for 15 to 30 minutes to allow the complexes to form. The TransIT-X2:miRNA complexes were added drop-wise in circular motions to ensure that all cells were covered by the mixture. The 6-well plate was rocked back and forth and side to side to evenly distribute the TransIT-X2 and miRNA mimics/inhibitor complexes onto the cultured cells. The transfected cells were cultured for 16 to 24 hours prior to medium change or serum starvation. All miRNA inhibitors or mimics and respective negative controls were purchased from Sigma-Aldrich.

Generation of NCKAP1 Short Hairpin RNA Lentivirus and NCKAP1 Stable Knockdown Cell Lines

NCKAP1 short hairpin RNA (shRNA) lentiviral particles were produced using MISSION shRNA NCKAP1 plasmids DNA (SHCLNG-NM_016965, MISSION shRNA Bacterial Glycerol Stock; Sigma-Aldrich) according to protocol provided. The shRNA nontargeting control vector (SHC002) was used as a negative control. Briefly, 293T cells were transfected with the lentiviral vector and the packaging plasmids pCMV-dR8.2 and pCMV-VSV-G (both obtained from Addgene) using TransIT-X2 transfection reagent (Geneflow Ltd), according to the manufacturer's instructions. The supernatant containing the lentivirus was harvested 48 hours later, filtered, aliquoted, and stored at −80°C. The p24 antigen ELISA (Zeptometrix) was used to determine the viral titer. The transducing unit was calculated using the conversion factor recommended by the manufacturer (10^4 physical particles per pg of p24 and 1 transducing unit per 10^3 physical particles for a VSV-G pseudotyped lentiviral vector), with 1 pg of p24 antigen converted to 10 transducing units. shRNA lentiviral infection and NCKAP1 stable knockdown cell line generation were performed as described in our previous studies with some modifications.[31–33] Briefly, VSMCs were plated 24 hours prior to infection in 6-well plates at 37°C. One transducing unit per cell (or $2–3\times10^5$ per well) of shRNA or control virus was added with 10 μg/mL hexadimethrine bromide (H9268; Sigma-Aldrich). Viral constructs were incubated for 24 hours with the cells before the media was replaced with complete media containing 4 μg/mL puromycin (P9620; Sigma-Aldrich). For selection of transductants, fresh media containing puromycin was added at 2- to 3-day intervals for 10 days. Stably infected cells were split and frozen for future experiments.

Cotransduction of NCKAP1 shRNA Lentivirus and miR-214 Inhibitor

For miR-214 inhibitor and NCKAP1 shRNA lentivirus cotransfection, VSMCs infected with nontarget or NCKAP1 shRNA lentivirus were transfected with miR-214 inhibitor or control miRNA inhibitor (25 nmol/L), as indicated in the Figure 6, using TransIT-X2 transfection reagent (Geneflow Ltd), according to the manufacturer's instructions. All procedures were same as the single-miRNA transfection except that the VSMCs were infected with nontarget or NCKAP1 shRNA virus, as described in the previous section.

NCKAP1 3′UTR Clone and miR-214 Binding Site Mutation

Reporter vector harboring sequences of the murine *NCKAP1* was created using cDNA from VSMCs. The flanking 3′UTR (3605nt–4403nt) of the murine *NCKAP1* gene (NM_016965.3) (Figure S1A) was amplified by polymerase chain reaction (PCR) with primers shown in Table S1 and cloned into the Sac I and Hind III sites of the pmiR-reporter-basic vector (Thermo Fisher Scientific Inc), designated as pmiR-Luc-NCKAP1-WT.

The miR-214 binding site 1, 2, or 3 mutations alone or combination were introduced into pmiR-Luc-NCKAP1-WT using the QuikChange site-directed mutagenesis kit (Agilent Technologies), according to the manufacturer's instructions. These were designated as pmiR-Luc-NCKAP1-BS1^{mut}, pmiR-Luc-NCKAP1-BS2^{mut}, pmiR-Luc-NCKAP1-BS3^{mut}, and pmiR-Luc-Notch1-BS1/2/3^{mut} mutants, respectively.

All vectors were verified by DNA sequencing.

Generation of KLF14 and SMYD5 3′UTR Reporters and Mouse miR-214 Gene Promoters

Reporter vectors harboring sequences of the murine Krüppel-like factor 14 (*KLF14*) and SET and MYND domain containing 5 (*SMYD5*) were created using cDNA from VSMCs. The flanking 3′UTR of the murine *KLF14* gene (NM_001135093; 3′UTR: 1272nt–2970nt) or *SMYD5* (NM_144918; 3′UTR: 1281nt–2491nt) gene was amplified by PCR with primers shown in Table S1 and cloned into the Sac I and Hind III sites of the pmiR-reporter-basic vector (Thermo Fisher Scientific Inc), designated as pmiR-Luc-KLF14 and pmiR-Luc-SMYD5, respectively.

The reported functional full length (−640:0) and the truncated (−640:−357) form of miR-214 gene promoters[34] were recovered from mouse genomic DNA by PCR using the respective primers shown in Table S1. Amplified DNA

fragments were cloned into the Sac I and Hind III sites of the pGL3-basic vector (Promega), designated as pGL3-miR-214_FL and pGL3-miR-214-short, respectively.

All vectors were verified by DNA sequencing.

Transient Transfection and Luciferase Assay

Luciferase assays for various gene 3′UTR reporters were conducted as described in our previous studies.[8,23,29,30,32] Briefly, VSMCs were cotransfected with an individual reporter gene (pmiR-Luc-NCKAP1-WT, pmiR-Luc-NCKAP1-BS1^{mut}, pmiR-Luc-NCKAP1-BS2^{mut}, pmiR-Luc-NCKAP1-BS3^{mut}, pmiR-Luc-Notch1-BS1/2/3^{mut}, pmiR-Luc-KLF14, pmiR-Luc-SMYD5, or pmiR-Luc-Notch1; 0.15 μg/2.5×10^4 cells) and control or miR-214 (or miR-34a) mimics (25 nmol/L) using TransIT-X2 transfection reagent (Geneflow Ltd), according to the manufacturer's instructions. pmiR-Luc-β-gal (0.20 μg/2.5×10^4 cells) or Renilla plasmid (15 ng/well) was included in all transfection assays as an internal control. Luciferase, Renilla, and/or β-galactosidase activities were detected 48 hours after transfection using a standard protocol. The relative luciferase unit was defined as the ratio of luciferase versus β-galactosidase or Renilla activity with that of the control (set as 1.0).

VSMC Proliferation Assays

Cell counting

Cell counting was conducted as described previously.[8] VSMCs were plated (1×10^5 per well) and cultured in 6-well plates precoated with 0.04% gelatin and supplemented with complete culture medium containing DMEM, 10% FBS, and 1% penicillin/streptomycin-glutamine. The plates were placed in humidified incubators at 37°C and 5% CO_2. After culturing for 24 hours, the cells were transfected with single miR-214 mimics/inhibitor or cotransduced with miR-214 inhibitor/NCKAP1 shRNA or respective negative control, as indicated in the Figures 2, 3, 5, and 6. After 12 to 16 hours of transfection, the cells were starved by culturing them in the DMEM supplemented with 1% penicillin/streptomycin-glutamine and 0.5% serum for another 24 hours. After the starvation process, the cells were treated with 20% FBS or PDGF-BB (10 ng/mL) for 48 hours before trypsinizing and manually counting the cells under a hematocytometer.

Bromodeoxyuridine incorporation assay

The 5-bromo-2′-deoxy-uridine (BrdU) incorporation assays were conducted as described previously.[8] VSMCs were transfected as described earlier and were recultured (0.75×10^4 per well) in 96-well plates overnight, followed by serum starvation for 24 hours. Starved VSMCs were restimulated with 20% FBS or 10 ng/mL PDGF-BB, respectively, for 48 hours. Cell proliferations were evaluated using the BrdU Labeling and Detection Kit II (Roche), according to the manufacturer's instructions. Briefly, cells were incubated with BrdU at a final concentration of 10 μmol/L for 8 to 12 hours before measurement. After fixation, cellular DNA was digested by nuclease and labeled with a peroxidase-conjugated BrdU antibody, followed by incubation with the peroxidase substrate. The absorbance of the samples was measured by a microplate reader at 405 nm (OD405) with reference measurement at 490 nm (OD490). Absorbance ($A_{405\ nm}-A_{490\ nm}$) values representing cell-proliferation ability were compared among treatments.

VSMC Migration Assays

Wound healing (scratch model)

Scratch wound healing assays were carried out using a previously described method.[8,35] In brief, VSMCs were cultured on 12-well plates overnight and transfected with miR-214 mimics, miR-214 inhibitor, or respective miRNA-negative control, as described earlier. After 12 to 16 hours of transfection, the confluent cells were starved by culturing them in the DMEM supplemented with 1% penicillin/streptomycin-glutamine and 0.5% serum for another 24 hours. After the starvation process, the cells were treated with hydroxyurea (2 mmol/L) to inhibit cell proliferation for 2 hours before subjecting them to 20% FBS or PDGF-BB (10 ng/mL) treatment. The cells were scratched in a crisscrossed manner and rinsed with PBS or DMEM 3 times to remove cell debris, followed by cultured in DMEM supplemented with 20% FBS or PDGF-BB (10 ng/mL) in the presence of 2 mmol/L hydroxyurea. The observations were made, and photomicrographic images were taken at 0 and 24 hours. Two experienced investigators blinded to the treatments used ImageJ software (National Institutes of Health) to measure the denuded cell surface of each wound (crisscrossed), and the percentages of cell closures (migrated area) were calculated as the difference in denuded area between hour 0 (A0) and hour 24 (A24) over the denuded area at hour 0 ×100: (A0−A24)/A0×100.

Transwell migration assay

Transwell migration assay was conducted as described previously.[8] VSMCs were transfected with miRNA (mimics or inhibitor), NCKAP1 shRNA, and/or their respective control, as indicated in the Figures 2, 3, 5 and 6. Transfected cells were cultured in DMEM containing 0.5% serum for 24 hours and harvested by trypsinization. An aliquot (250 000 cells/200 μL) of the cells in serum-free DMEM was dispensed into the transwell inserts (8-μm pore size, item number 662638; Greiner Bio-One Ltd) precoated with 0.5% gelatin (G1393; Sigma-Aldrich), and DMEM (600 μL) with 20% FBS or 30 ng/mL PDGF-BB was placed in the lower chamber. The transwell plates were incubated

at 37°C in a 5% CO_2 incubator for 18 to 24 hours. Nonmigrated cells in the top insert were carefully removed by cotton swab, and the migrated cells in the bottom side were stained with crystal violet dye. Images were captured at 5 fixed locations (right, bottom, left, up, and center), and migrated cells were counted by 2 experienced investigators blinded to the treatments.

Immunoblotting

Cells were harvested and lysed in lysis buffer (50 mmol/L Tris-Cl, pH 7.5; 150 mmol/L NaCl; 1 mmol/L EDTA, pH 8.0) supplemented with protease inhibitors and 0.5% Triton and sonicated to obtain whole-cell lysate. Next, 40 μg of protein was separated by SDS-PAGE with 4% to 20% Tris-Glycine gel (Invitrogen) and subjected to standard Western blot analysis. In some experiments, the blots were subjected to densitometric analysis with ImageJ software. Relative protein expression level was defined as the ratio of target protein expression level to GAPDH expression level with that of the control sample set as 1.0.

Indirect Immunofluorescent Staining for Cells

For detecting Ki-67–positive cells, cells subjected to various treatments were fixed and labeled with antibody against Ki-67 (Abcam) or rabbit isotype immunoglobulin G control and visualized using a donkey anti–rabbit immunoglobulin G antibody conjugated with CF 568 fluorescence (in 1:400 dilution; Sigma-Aldrich). For phalloidin-FITC staining alone, another setting of cells with different treatments, as indicated in the Figures 5 and 6, was fixed and labeled with phalloidin-FITC (P5282), according to the manufacturer's instructions. For double-immunofluorescent staining with NCKAP1 and phalloidin-FITC, a separate setting of cells with different treatments, as indicated in the Figures 5 and 6, was fixed and labeled with anti-NCKAP1, or rabbit isotype immunoglobulin G control. Next, cells were visualized using a donkey anti–rabbit immunoglobulin G antibody conjugated with CF 568 fluorescence (in 1:400 dilution; Sigma-Aldrich) and phalloidin-FITC (P5282), according to the manufacturer's instructions. Cells were counterstained with DAPI (4′,6-diamidino-2-phenylindole; Sigma-Aldrich) and mounted in Fluoromount-G (Cytomation; Dako). Images were examined using an SP5 confocal microscope and Leica TCS Sp5 software (Leica) at room temperature and were processed with Photoshop software (Adobe).

Reverse Transcriptase–Quantitative PCR for mRNA and miRNAs

Real-time quantitative PCR (RT-qPCR) was performed as described previously.[8,23,29,30,36] Briefly, total RNAs containing small RNAs (miRNAs) were extracted from cells using the mirVana Protein and RNA Isolation System Kit (Thermo Fisher Scientific Inc) or TRI reagent (Sigma-Aldrich), according to the manufacturer's instructions, and subjected to DNase I (Sigma-Aldrich) digestion to remove potential DNA contamination. Reverse transcription for long RNA was performed using an Improm-II RT kit (Promega) with RNase inhibitor (Promega) and Random primers (Promega). The NCode VILO miRNA cDNA Synthesis Kit (A11193-051; Thermo Fisher Scientific Inc) was used to synthesize poly(A) tails of all the miRNAs followed by cDNA synthesis from the tailed population in a single reaction. The resultant cDNA was diluted to a working concentration of 5 ng/μL and stored at −20°C. NCode EXPRESS SYBR GreenER qPCR SuperMix Universal (Thermo Fisher Scientific Inc) was used in miRNA RT-qPCR. Relative mRNA or miRNA expression level was defined as the ratio of target gene expression level or miRNA expression level to 18S or U6 small nuclear RNA expression level, respectively, with that of the control sample set as 1.0. In some experiments, relative mRNA or miRNA expression level was defined as the ratio of target gene expression level or miRNA expression level to 18S or U6 small nuclear RNA expression level, respectively. Primers were designed using Primer Express software (Thermo Fisher Scientific Inc); and the sequence for each primer is listed in Table S1.

Proteomics Studies

Sample preparation for proteomic analysis

VSMCs transfected with control or miR-214 mimics were directly lysed in a urea-based lysis buffer (8 mol/L urea in 20 mmol/L HEPES, pH 8.0; 1 mmol/L Na_3VO_4, 1 mmol/L NaF, 0.5 mmol/L β-glycerol phosphate, and 2.5 mmol/L $Na_2H_2P_2O_7$), and proteins were digested using trypsin, as reported previously.[37,38] The enriched peptides were subjected to the following analyses, as described in our previous study.[39,40]

Mass spectrometry

Protein-derived peptides were analyzed by the LTQ Orbitrap XL mass spectrometer (Thermo Fisher Scientific Inc) coupled with a nanoAcquity liquid chromatography system (Waters). Peptide separation was performed using solution A (0.1% formic acid in liquid chromatography and mass spectrometry [MS]–grade water) and solution B (0.1% formic acid in liquid chromatography–MS acetonitrile) as mobile phases. Gradient runs from 2% to 30% solution B in 100 minutes and from 30% to 60% in 10 minutes were followed by a final 10-minute wash at 85% solution B.

Full MS scans were acquired in the Orbitrap mass analyzer over the range m/z 375 to 1500 with a mass resolution of 30 000. Tandem MS (MS/MS) was acquired using top 7 data-

dependent acquisition with high-energy collision dissociation (40%). The gas-phase fractionation method was applied to acquire MS/MS scans.

Peptide identification by database search

MS/MS data were converted to Mascot generic format files using Mascot Distiller (version 2.2; Matrix Science) and searched against the 2012_03 databases of UniProt and SwissProt using the Mascot search engine (version 2.2). Significance of peptide identification was assessed by comparing results returned by searches against random and forward databases. Fold discovery rates at several cutoff values of Mascot scores and mass tolerances were used to calculate an empirical value of probability of random identification.

Data analysis and volcano plot analysis

Relative quantification of peptides across experimental conditions was achieved by comparing peak heights of extracted ion chromatograms (automated by Pescal), as described previously.[37,40] The data were normalized to the sum of all intensities derived from a sample (columns). When comparing the effects of miR-214 overexpression on protein regulation, peptide signals were divided by those of the untreated control samples (control miRNA mimics). The *P* values of differences across treatments were obtained by means of a *t* test of $\log_2$-transformed fold changes, and these were adjusted for multiple testing through the Benjamini–Hochberg procedure, as described previously.[37] The fold change was transformed using the $\log_2$ function, so the data are centered around zero, whereas the Benjamini–Hochberg corrected *P* value was $-\log_{10}$ transformed for volcano plot analysis.

Mouse Femoral Artery Denudation Injury and miR-214 Agomir Perivascular Delivery

C57BL/6 mice were anesthetized, and the surgical procedure was similar to that described previously.[8,24,41,42] Removal of the endothelium of the femoral arteries was achieved by 3 to 5 passages of a 0.25-mm angioplasty spring wire (tips of cross-IT 200× guide wire; Abbott Laboratories). After the vascular injury, the injured femoral arteries were randomly received miR-214 or Cel-miR-67 agomir treatments, as described in our previous study.[8] Briefly, after injury, 100 μL of 30% pluronic gel containing chemically modified and cholesterol-conjugated 2.5 nmol miR-214 or scramble (Cel-miR-67) agomirs was applied perivascularly to injured femoral arteries. The micrON miRNA agomirs were purchased from RiboBio (Guangzhou RiboBio Co, Ltd). The in vivo expression efficiency and stability of such agomirs have been documented extensively by many research groups worldwide.[8,43–46] Additional femoral arteries were harvested at 3 days (for gene expression) or 14 days (for protein expression) after injury (3–5 femoral arteries from each group were pooled for each independent experiment, and triplicate experiments were conducted). Total RNAs including small RNAs and proteins were extracted for RT-qPCR or Western blotting analysis of miR-214, NCKAP1, or PCNA gene/protein expression in injured vessels. Our previous study[8] showed that perivascular delivery of 2.5 nmol agomirs into each injured vessel generally resulted in 5 to 10 times higher expression levels compared with control mice (received Cel-miR-67 agomirs) or normalized target miRNA expression levels in injured arteries to levels similar to those in normal uninjured vessels. All animal experiments were performed according to the Animals (Scientific Procedures) Act of 1986 (United Kingdom), and all protocols were approved by the Institutional Committee for Use and Care of Laboratory Animals. In addition, the principles governing the care and treatment of animals, as stated in the Guide for the Care and Use of Laboratory Animals published by the National Academy of Sciences (8th ed., 2011), were followed at all times during this study. All mice were euthanized by placing them under deep anesthesia with 100% O_2 and 5% isoflurane, followed by decapitation.

Morphometric Analysis and Quantification of Lesion Formation

All procedures used in this study were similar to those described in our previous study.[8] Briefly, the femoral arteries (≈1.0 mm from injury site) were harvested 4 weeks after the operation. The specimens were fixed in 4% formaldehyde for hematoxylin and eosin staining. Sections (8 μm) were collected at 100-μm intervals (10 sections per interval), mounted on slides, and numbered. Six digitized sections with same identification number from 3 segments/intervals (≈0.4, 0.5, and 0.6 mm from injury site) of each animal (eg, IV-1/2, V-1/2, VI-1/2 represent the first and second sections of the fourth, fifth, and sixth segment/interval, respectively) were stained with hematoxylin and eosin for morphometric analysis. The procedure used for lesion quantification was similar to that described previously.[8,24,41,42] Briefly, external elastic membrane, internal elastic membrane, lumen, media, and neointimal areas were automatically measured on hematoxylin and eosin–stained cross-sectional femoral artery segments using a computerized image analysis system (pixel^2, a unit of area measurement, AxioVision software; Zeiss) by 2 experienced investigators blinded to the treatments. Six sections were analyzed per vessel sample and averaged.

Statistical Analysis

Results are presented as Mean±SEM. Statistical analysis was performed using GraphPad Prism5 (GraphPad Software). The Shapiro–Wilk normality test was used for checking the

normality of the data. Data with a Shapiro–Wilk test $P>0.05$ was considered to fit a normal distribution. A 2-tailed unpaired Student *t* test was used for comparisons between 2 groups, and a 1-way ANOVA test with a Bonferroni post hoc test was applied when >2 groups were compared if the data displayed a normal distribution. An $\alpha=0.05$ was chosen as the significance level, and *P* values of <0.001, <0.01, and <0.05 were considered statistically significant.

Results

miR-214 Expression in VSMCs is Significantly Downregulated by Various Pathogenic Stimuli

Extensive studies[9,25–28] have suggested that VSMC proliferation and migration can be promoted by various pathogenic stimuli including high concentration of serum (20%), PDGF-BB, oxidized low-density lipoprotein, or its components such as 4-hydroxynonenal and 7-ketocholesterol.[47] To study whether miR-214 expression was regulated on such atherogenic stimulation, serum-starved VSMCs were treated with various stimuli and harvested at different time intervals. As expected, both PDGF-BB and 20% serum significantly inhibited miR-214 expression from 3 to 24 hours of treatment compared with expression of untreated cells (at 0 hour) (Figure 1A). Although not reaching a significant level, a decreasing trend was also observed at 48 hours with both treatments (Figure 1A). A similar effect was observed with 4-hydroxynonenal and 7-ketocholesterol treatment (Figure 1C), suggesting a role for miR-214 in VSMC proliferation and migration.

To further study whether serum and PDGF-BB downregulate miR-214 expression in human VSMCs, similar experiments were conducted in human aortic SMCs. RT-qPCR data showed that miR-214 expression levels were significantly downregulated by both serum and PDGF-BB in human aortic SMCs (Figure 1B), confirming a similar regulatory effect of serum and PDGF-BB on miR-214 expression in human VSMCs.

PDGF-BB and Serum Downregulates miR-214 in VSMCs By Inhibiting the Transcription Factor Twist-1

It is well known that miRNA synthesis and maturation is under 2 molecular controls: transcription and biogenesis. To differentiate these 2 mechanisms, we initially conducted RT-qPCR analyses with specific primers to examine the miR-214 primary transcript. RT-qPCR data showed that the expression level of primary miR-214 was significantly downregulated by serum and PDGF-BB (Figure 1D), indicating that miR-214 was regulated by PDGF-BB and serum at the transcriptional level. It has been reported that miR-214 expression is regulated by transcription factor Twist-1 via an E-box promoter element during development[34]; therefore, we wondered if a similar mechanism were responsible for miR-214 inhibition by serum and PDGF-BB. To this end, we generated 2 mouse miR-214 gene promoters, pGL3-miR-214-FL and pGL3-miR-214-short (Figure 1E), using a strategy similar to that reported by Lee et al.[34] Data from luciferase activity assays showed that the luciferase activity was significantly decreased by serum (Figure 1F) and PDGF-BB (Figure 1G) in VSMCs transfected with pGL3-miR-214-FL, whereas no such inhibitory effect was observed in VSMCs transfected with pGL3-miR-214-short reporter lacking the E-box. These data demonstrate that various pathogenic stimuli regulate miR-214 expression in VSMCs through a transcriptional mechanism, and the E-box element is required for such regulation. As expected, the expression level of *Twist-1* was dramatically downregulated by serum and PDGF-BB (Figure 1H), suggesting that these 2 pathogenic stimuli downregulate miR-214 expression in VSMCs by inhibiting the transcription factor Twist-1.

VSMC Proliferation and Migration Are Inhibited by miR-214

VSMC proliferation and growth and accumulation within intima have been recognized as major events during the early stage of atherosclerotic lesion formation and postangioplasty restenosis. We wondered if miR-214 could play a role in VSMC proliferation. For such a purpose, VSMCs were transfected with miR-214 mimics and subjected to BrdU incorporation analyses and cell counting, respectively, to evaluate the potential effects of miR-214 overexpression on VSMC proliferation. As expected, miR-214 expression in VSMCs was significantly increased by miR-214 mimics (Figure 2A). Importantly, data from BrdU incorporation assays (Figure 2B) and cell counting (Figure 2C) showed that serum- and PDGF-BB–induced VSMC proliferation was significantly inhibited by miR-214 overexpression. To further confirm the role of miR-214 in VSMC growth, miRNA loss-of-function experiments were conducted in VSMCs cultured under similar conditions using miR-214 inhibitor. Data shown in Figure 2F revealed that the endogenous miR-214 expression level in VSMCs was successfully inhibited by miR-214 inhibitor. Consistent with the findings from miR-214 gain-of-function experiments, miR-214 inhibition in VSMCs significantly increased PDGF-BB– and serum-induced cell proliferation, respectively (Figure 2G and 2H), suggesting that miR-214 plays an important role in VSMC growth.

VSMC migration into intima is another key determining factor for atherosclerotic lesion formation and postangioplasty restenosis. To examine whether miR-214 also plays a role in VSMC migration, VSMCs were transfected with miR-214 mimics, inhibitor, or their respective negative controls, followed by cell migration assays in response to serum or PDGF-BB

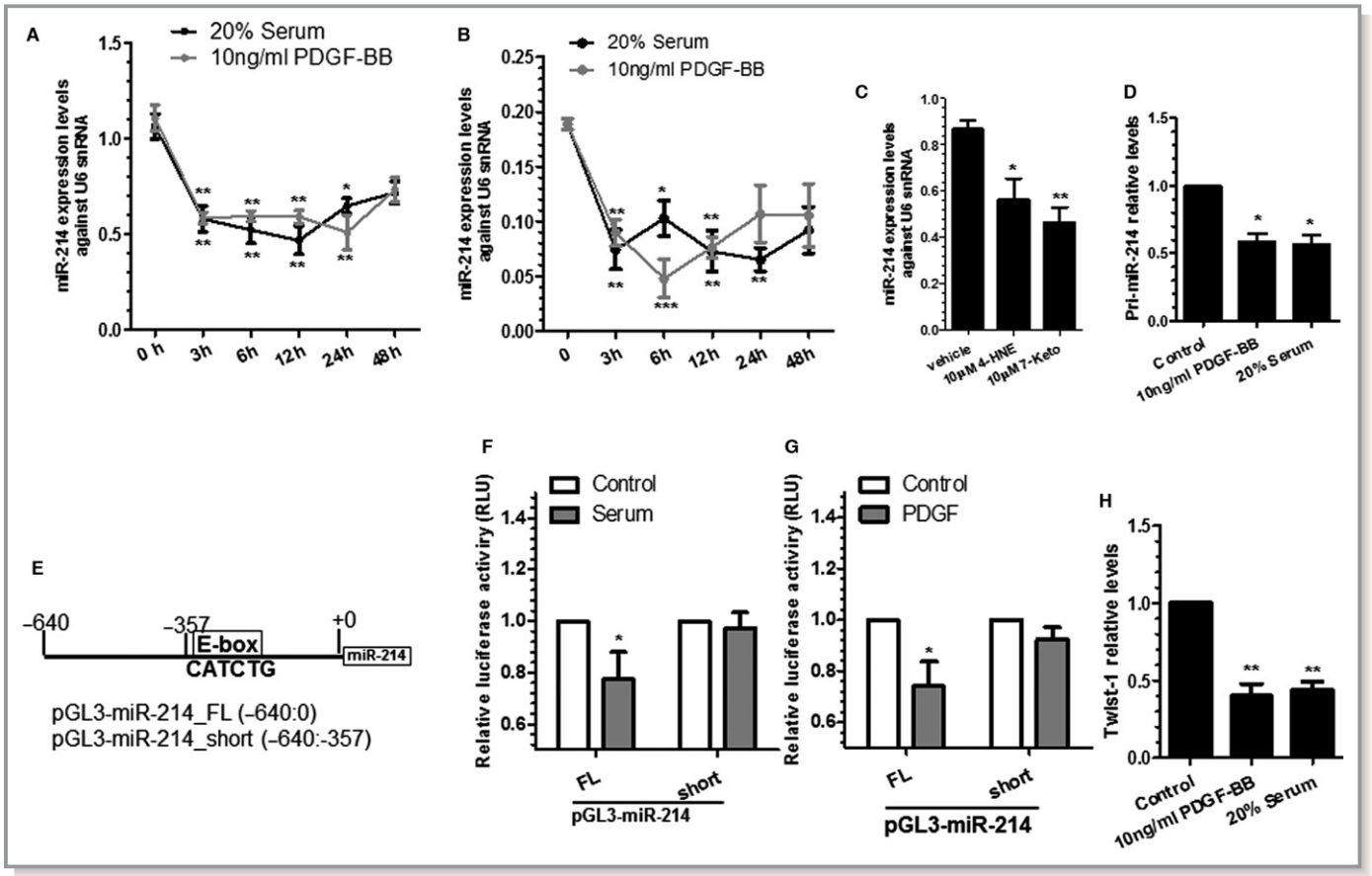

Figure 1. Transcriptional inhibition of miR-214 by different pathogenic stimuli in vascular smooth muscle cells (VSMCs). A through C, MicroRNA miR-214 is regulated by various pathogenic stimuli. Murine VSMCs (A and C) and human aorta smooth muscle cells (hAoSMCs) (B) were subjected to serum starvation for 24 hours, followed by different stimuli, as indicated. Total RNAs were harvested at indicated times (10 ng/mL platelet-derived growth factor BB [PDGF-BB]/20% serum) (A and B) or at 24 hours for 4-hydroxynonenal (4-HNE) and 7-ketocholesterol (7-Keto) treatments (C) and subjected to reverse transcriptase–quantitative PCR (RT-qPCR) analyses. Data are presented as mean±SEM (circles and error bars, respectively) in (A and B) or as mean+SEM (bars plus error bars) in (C) of 5 independent experiments (n=5). *<0.05, **<0.01, and ***<0.001; different treatments were compared with 0 hour (A and B) or vehicle (C). D, Serum and PDGF-BB downregulate miR-214 primary transcript. Serum-starved VSMCs were incubated with serum and PDGF-BB for 3 hours. Total RNAs were harvested and subjected to RT-qPCR analyses. E, A schematic diagram of mouse miR-214 gene promoter reporters. F and G, The E-box element is required for miR-214 gene inhibition by serum and PDGF-BB. VSMCs transfected with respective reporters harboring the full length (pGL3-miR-214-FL; −640:0) or truncated form (pGL3-miR-214-short; −640:−357, lacking E-box element) of the miR-214 gene promoter were subjected to serum starvation for 24 hours, followed by incubation with 20% serum (F) or 10 ng/mL PDGF-BB (G) for 3 hours, respectively. Cell lysate was harvested and subjected to luciferase activity assays. H, Twist-1 expression is inhibited by serum and PDGF-BB in VSMCs. cDNA samples generated in (D) were used to examine Twist-1 expression level by RT-qPCR. Data are presented as mean+SEM (bars plus error bars) of 3 (D and H) or 6 (F and G) independent experiments (n=3 or n=6). *<0.05, **<0.01, and ***<0.001, compared with vehicle control. FL indicates full length; RLU, relative luciferase unit; snRNA, small nuclear RNA.

stimulation, respectively. Decreased cell migratory capacity was observed in the VSMCs transfected with miR-214 mimics in response to both PDGF-BB and serum stimulation, as demonstrated in wound healing (Figure 2D) and transwell migration assays (Figure 2E), respectively, compared with the control cells. As expected, the migratory ability of cells transfected with miR-214 inhibitor was clearly greater than that of control cells (Figure 2I and 2J), supporting a role for miR-214 in regulating VSMC migration.

To investigate whether miR-214 also plays a pathological role in human VSMCs, miR-214 inhibitor and control miR inhibitor were transfected into human aortic SMCs. Our data showed that human aortic SMC proliferation and migration were significantly enhanced by miR-214 inhibition (Figure 3A) in response to serum or PDGF-BB stimulation, as demonstrated in BrdU incorporation (Figure 3B) and transwell migration (Figure 3C) assays, respectively, inferring a role for miR-214 in human pathology.

Proteomics Analysis to Uncover the Potential Target Genes of miR-214 in VSMCs

In searching the potential target genes of miR-214 in VSMCs, total proteins were harvested from VSMCs transfected with

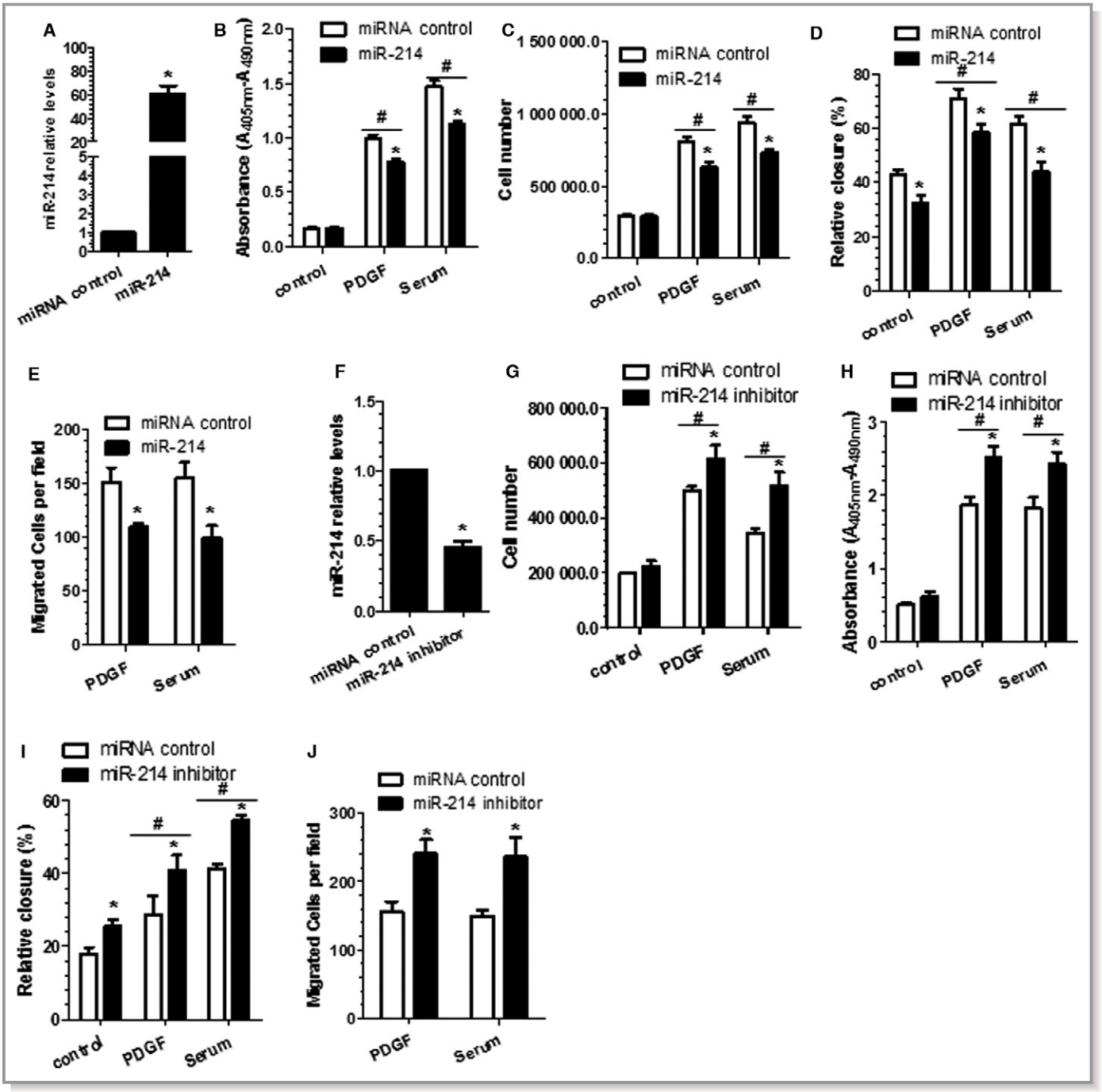

Figure 2. Vascular smooth muscle cell (VSMC) proliferation and migration are modulated by miR-214. miR-214 mimics (miR-214) (A through E) and inhibitor (miR-214 inhibitor) (F through J) or respective control microRNAs (miRNAs) were transfected into VSMCs, followed by 24 hours of serum starvation. Serum-starved cells were treated with platelet-derived growth factor BB (PDGF-BB) or serum for another 48 hours, followed by bromodeoxyuridine incorporation assays (B and H) or cell counting (C and G). In another setting of experiments, serum-starved cells were subjected to wound-healing assays (D and I) or transwell migration analyses (E and J) in response to PDGF-BB or serum stimulation for another 24 hours, respectively. Meanwhile, cells were harvested to examine the miR-214 expression levels by reverse transcriptase–quantitative PCR analyses (A and F). Note that in the transwell migration experiments, only a few cells were migrated through the insert without any chemoattractant. In the wound-healing assays, the percentage of cell closure or migrated area was calculated as described in the Materials and Methods section. Data are presented as mean+SEM of 3 to 4 independent experiments (n=3–4). *<0.05 (miR-214 mimics or inhibitor vs miRNA control within respective treatment). #<0.05 (Compared PDGF/serum with control, with or without miR-214 modulation).

control and miR-214 mimics and subjected to label-free quantitative proteomics analyses. miR-214 overexpression in VSMCs transfected with miR-214 mimics was confirmed using RT-qPCR (Figure 4A). By applying 25% of change as the cutoff value, 219 proteins were found to be modulated by miR-214 overexpression (Table S2). Among them, 59 and 160 proteins were downregulated and upregulated, respectively, by miR-214. Because it has been widely accepted that miRNAs mainly function in RNA silencing and posttranscriptional regulation of target gene expression, the proteins that were downregulated by miR-214 overexpression in VSMCs represent the potential direct target genes of miR-214. Interestingly, Gene Ontology (GO) term enrichment analysis of the downregulated proteins showed that actin filament polymerization was the highest enriched functional/biological process and was inhibited by miR-214 overexpression in VSMCs (Table S3). More specifically, we observed that most of these downregulated proteins (28 of 59) (yellow-highlighted proteins in Table S2) are under the GO terms of 'regulation of cell migration' (eg, NCKAP1, EMAL1, ARPC2, LIMS2, SPI2), 'proliferation' (eg, EMAL1, LIMS2, LTOR3), 'adhesion' (eg, SNX5, SNX12, LIMS2), 'actin filament reorganization and actin polymerization' (eg, NCKAP1, ARPC2, CAPZB), 'cell cycle' (eg, APC7, ARL3, ULA1), and 'gene expression' (eg, KLF14, SMYD5, LONM), respectively, further confirming a role of miR-214 in VSMC proliferation and migration. Importantly, by utilizing several computational algorithmic databases, such as RNA22 (https://cm.jefferson.edu/rna22/), DIANA-microT-CDS (http://diana.imis.athena-innovation.gr/DianaTools/index.php?r=MicroT_CDS/index), TargetScan7.1 (http://www.targetscan.org/mmu_71/), miRanda-rel2010 (http://www.microrna.org/microrna/getGeneForm.do), and miRDB4.0 (http://mirdb.org/cgi-bin/search.cgi), we identified ≥1 miR-214 binding site within the 3′UTR of 39 (of 59) genes with protein expression levels that were decreased by miR-214 overexpression. As such, these proteins likely represent good candidates as the functional direct target genes of miR-214 in VSMCs.

NCKAP1 Identified as a Functional Target of miR-214 in VSMCs

It is unrealistic to assess whether all identified 39 downregulated genes with predicted miR-214 binding sites are direct target genes of miR-214 in the current study. Consequently, a volcano plot was applied to quickly identify the most meaningful changes in our large proteomics data sets composed of replicate data. As shown in the volcano plot (Figure 4B), with stringent criteria and $P<0.05$, NCKAP1 (also named as NAP1 or NAP125) was clearly identified as the most meaningful and important target gene of miR-214 in VSMCs. Data from Western blot analyses (Figure 4C) confirmed the proteomics data that the NCKAP1 protein level was significantly downregulated by miR-214 overexpression. Unsurprisingly, 3 miR-214 binding sites (binding site 2 is predicted to be highly conserved across >10 species including human, whereas binding sites 1 and 3 are conserved in mouse and rat) were found within the 3′UTR of *NCKAP1* using computational algorithms, DIANA-microT/RNA22 (Figure S1A). Moreover, a favorable minimum loop-free energy (dH: −136.5, −143.1 and −150.2 kcal/mol for binding site 1, 2 and 3, respectively) in the formation of the miR-214:*NCKAP1* 3′UTR duplex stem loop for all 3 binding sites was observed by using mFold software (http://mfold.rna.albany.edu/?q=DINAMelt/Two-state-melting) (Figure S1B). As expected, *NCKAP1* gene expression levels were significantly down- or upregulated by overexpression or inhibition, respectively, of miR-214 in VSMCs (Figure 4D and 4E). These data imply that NCKAP1 is negatively regulated by miR-214 directly or indirectly. To determine whether miR-214 can directly regulate NCKAP1, the 3′UTR of *NCKAP1* that contained the 3 miR-214 binding sites was cloned into a luciferase reporter. Data from our miRNA reporter assay showed that the activity of luciferase from construct harboring the wild-type *NCKAP1* 3′UTR was significantly inhibited by miR-214 overexpression (Figure 4F). Importantly, all 3 binding sites are important for *NCKAP1* 3′UTR reporter activity repression mediated by miR-214, as demonstrated in luciferase activity assays with miR-214 binding site single ($BS1^{mut}$, $BS2^{mut}$ or $BS3^{mut}$) or combination ($BS1/2/3^{mut}$) mutant reporters (Figure 4F). Taken together, these data demonstrated that NCKAP1 is a true mRNA target of miR-214 that is negatively regulated by miR-214 in VSMCs.

It is well known that 1 miRNA can target multiple target genes. To further assess whether any other candidate genes among the 39 downregulated genes with predicted miR-214 binding sites are also direct target genes of miR-214 in the context of VSMCs, the 3′UTRs of *KLF14* and *SMYD5*, which contained 2 and 4 miR-214 binding sites, respectively, were cloned into a luciferase reporter (pmiR-Luc). The reason for selecting KLF14 and SMYD5 in our validation experiment is that the KLF14 is an important transcriptional factor, whereas SMYD5 is a powerful epigenetic regulator with methyltransferase activity. The miRNA luciferase activity data showed that the luciferase activity of the construct harboring the *SMYD5* 3′UTR (Figure S2B), but not of the reporter containing the *KLF14* 3′UTR (Figure S2A), was significantly inhibited by miR-214 overexpression, confirming that SMYD5 is another target gene of miR-214.

We recently demonstrated that another miRNA, miR-34a, modulates VSMC functions and neointima formation through targeting the *Notch1* gene.[8] We wondered if there was cross-talk or overlap between miR-214 and miR-34a in terms of target gene regulation. To this end, we conducted cotransfection experiments (miR214 mimics and *Notch1* 3′UTR

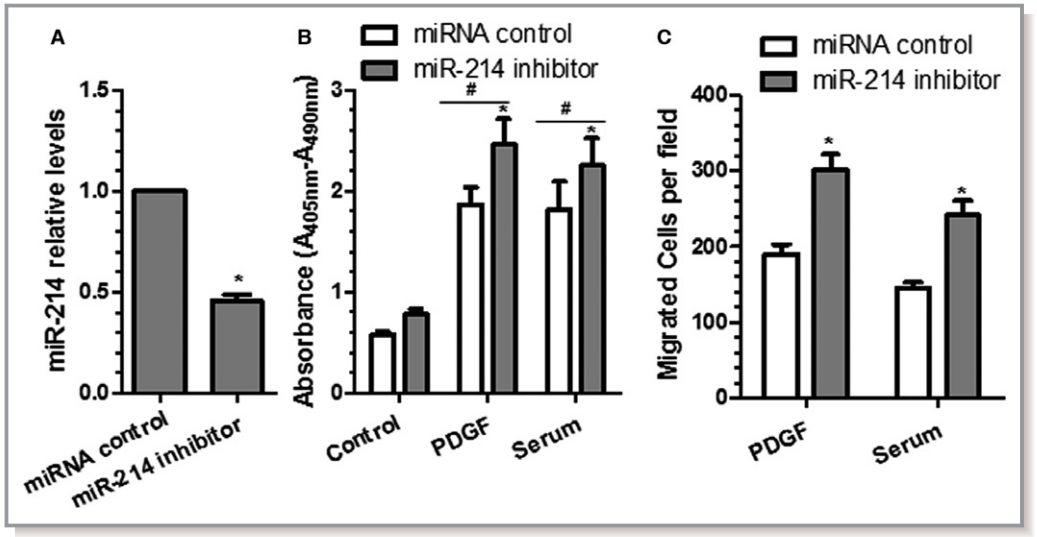

Figure 3. Inhibition of miR-214 increases human vascular smooth muscle cell (VSMC) proliferation and migration. miR-214 inhibitor or control microRNA (miRNA) inhibitor were transfected into human aorta smooth muscle cells, followed by 24 hours of serum starvation. Serum-starved cells were treated with platelet-derived growth factor BB (PDGF-BB) or serum for another 48 hours, followed by reverse transcriptase–quantitative PCR analyses to examine the miR-214 expression levels (A) and bromodeoxyuridine incorporation assays (B), respectively. In another set of experiments, serum-starved cells were subjected to transwell migration analyses (C) in response to 30 ng/mL PDGF-BB or 20% serum stimulation for another 24 hours. Mean+SEM of 3 independent experiments (n=3) is presented. *<0.05 (miR-214 inhibitor vs miRNA control within respective treatment); #<0.05 (PDGF/serum vs control, with or without miR-214 modulation).

reporter; miR34a mimics and *NCKAP1* 3′UTR reporter) in VSMCs. Data shown in Figure S2C and S2D revealed that neither the *Notch1* 3′UTR reporter activity nor that of *NCKAP1* was regulated by miR-214 or miR-34a, respectively, demonstrating that there is not cross-talk between these 2 miRNAs in the context of VSMCs.

NCKAP1 Knockdown in VSMCs Recapitulates the Effects of miR-214 Overexpression on Actin Polymerization, Cell Migration, and Proliferation

These data have demonstrated that NCKAP1 is the authentic mRNA target of miR-214 in VSMCs. Importantly, it has been reported that NCKAP1 is a constitutive and essential component of a WAVE2- and Abi-1–containing complex linking Rac to site-directed actin assembly and plays an essential role in regulation of cell migration through driving lamellipodia formation.[48] It is plausible that miR-214 could mediate VSMC migration and/or proliferation through modulating actin polymerization and/or lamellipodia formation by targeting NCKAP1. To support such a notion, we examined whether miR-214 overexpression affects actin polymerization and/or lamellipodia formation in VSMCs. Immunofluorescence staining with NCKAP1 antibody and phalloidin-FITC (a high-affinity F-actin probe conjugated to FITC) showed that typical lamellipodia was formed in VSMCs transfected with control miRNA mimics, whereas such a characteristic was less evident in VSMCs transfected with miR-214 mimics (Figure 5A). Compared with control cells, a much lower level of actin polymerization was observed in miR-214–overexpressing VSMCs, as shown with a much weaker F-actin staining intensity (Figure 5A). As expected, no or very low NCKAP1 expression was observed in VSMCs transfected with miR-214 mimics, further confirming that NCKAP1 expression is inhibited by miR-214. An NCKAP1-stable knockdown cell line was generated using NCKAP1 shRNA lentivirus to further evaluate and confirm a potential role of NCKAP1 in various VSMC functions. More than 60% of NCKAP1 inhibition efficiency was achieved in NCKAP1-stable knockdown VSMCs, as demonstrated with immunofluorescence staining (Figure 5B) and RT-qPCR (Figure 5C) assays, respectively. As expected, a similar phenomenon in terms of actin polymerization and/or lamellipodia formation was observed in NCKAP1-stable knockdown VSMCs (Figure 5B). Interestingly, NCKAP1 was observed to colocalize with F-actin within lamellipodia and membrane ruffles that face the direction of cell movement in the control cells, and such assembly was disrupted in the cells transfected with miR-214 mimics (Figure 5A) and infected with NCKAP1 shRNA lentivirus (Figure 5B), respectively. Importantly, compared with control

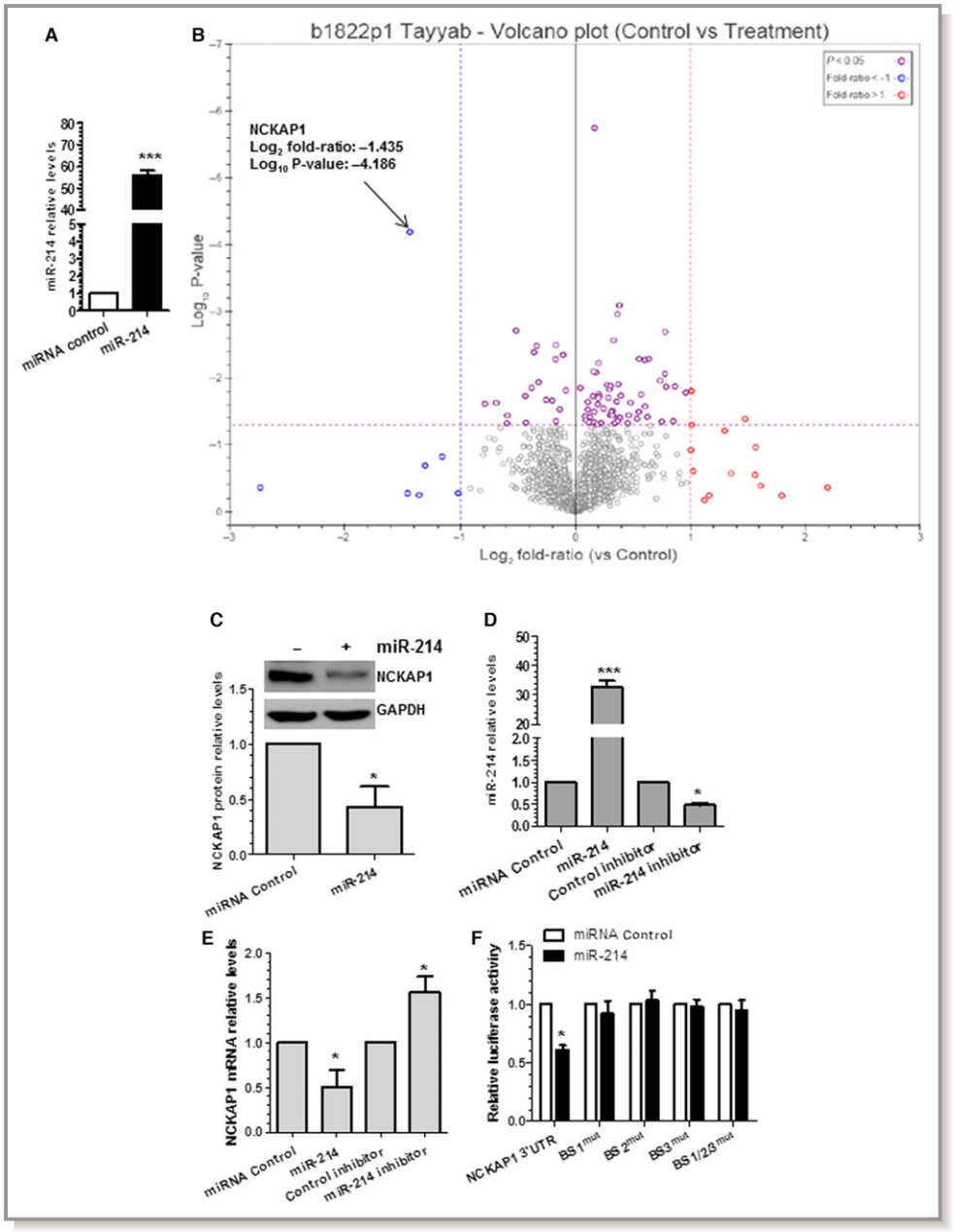

Figure 4. NCK associated protein 1 (NCKAP1) is the target gene of miR-214 in vascular smooth muscle cells (VSMCs). A through C, NCKAP1 protein level was significantly downregulated by miR-214 overexpression in VSMCs, as shown in the volcano plot (B), and confirmed by Western blot analyses (C). Reverse transcriptase–quantitative PCR (RT-qPCR) confirmed miR-214 overexpression in VSMCs (A). B, Volcano plot showing *P* values ($-\log_{10}$) vs protein ratio of miR-214 mimics/control mimics ($\log_2$) of all 1594 proteins fulfilling strict quantitation criteria (red, 14 upregulated proteins with 2-fold changes; blue, 7 downregulated proteins with 2-fold changes; purple, significantly changed but such change is <2-fold on miR-214 overexpression; ANOVA with $P<0.05$). D and E, Modulations of miR-214 expression levels in VSMCs negatively regulates *NCKAP1* gene expressions. VSMCs were transfected with miR-214 mimics (miR-214) or inhibitor or with respective negative controls. Total RNAs were harvested and subjected to RT-qPCR analyses with indicated primers. F, All 3 binding sites are important for miR-214–mediated *NCKAP1* gene repression. miR-214 mimics or negative control were cotransfected into VSMCs with wild-type *NCKAP1* 3′ untranslated region (3′UTR) reporter or the indicated single/combined binding site mutants (binding sites 1 [$BS1^{mut}$], 2 [$BS2^{mut}$], and 3 [$BS3^{mut}$] or the combinational mutations [$BS1/2/3^{mut}$]). Luciferase activity was measured at 48 hours after transfection. The data presented are representative (C) or show mean+SEM of 3 to 4 independent experiments (C through F). *<0.05, ***<0.001 Compared with miRNA control.

cells VSMCs transfected with miR-214 mimics or NCKAP1-stable knockdown VSMCs displayed much lower levels of cell proliferation and migration, as demonstrated in cell counting (Figure 5D), cell proliferation marker (Ki-67) staining (Figure 5E), and transwell migration (Figure 5F) analyses. Moreover, we observed no significant difference in terms of VSMC proliferation and migration between VSMCs transfected with miR-214 mimics and infected with NCKAP1 shRNA lentivirus (Figure 5C through 5F), confirming similar effects of miR-214 overexpression and NCKAP1 silencing on VSMC functions. Overall, these data suggest that NCKAP1 inhibition/repression in VSMCs can recapitulate the effects of miR-214 overexpression on actin polymerization, cell migration, and proliferation.

NCKAP1 Inhibition Is Required for miR-214 Mediation of VSMC Growth and Motility

To study whether NCKAP1 knockdown could ablate the promoting effects of miR-214 inhibition on VSMC functions, cotransduction experiments with miR-214 inhibitor, NCKAP1 shRNA lentivirus, and/or respective controls, as indicated in the figure 6, were conducted in VSMCs, followed by phalloidin-FITC staining, VSMC proliferation, and migration assays. RT-qPCR data showed that both miR-214 and *NCKAP1* were successfully downregulated by respective miR-214 inhibitor and NCKAP1 shRNA (Figure 6A). Moreover, the expression level of *NCKAP1* was upregulated by miR-214 inhibition, and such induction was abolished by *NCKAP1* knockdown in the presence of miR-214 inhibition (Figure 6A), further confirming that *NCKAP1* gene expression is regulated by miR-214. Importantly, the gene expression levels of *PCNA* (cell proliferation gene) with indicated treatment showed that miR-214 inhibition activated but NCKAP1 knockdown inhibited *PCNA* gene expression and that *PCNA* gene activation by miR-214 inhibition was blunted by NCKAP1 shRNA (Figure 6A). Proliferation assay data consistently showed that miR-214 inhibition or NCKAP1 knockdown alone in the VSMCs significantly increased or decreased VSMC proliferation, as demonstrated in cell counting (Figure 6B) and Ki-67 staining (Figure 6C1 and 6C2) assays, respectively; however, resuppression of NCKAP1 in the cells with miR-214 inhibition almost abolished the promoting effects of miR-214 inhibition on VSMC proliferation (Figure 6B and 6C), suggesting that miR-214 inhibits VSMC proliferation through repression of NCKAP1. Similar trends were observed in VSMC migration and actin polymerization, as demonstrated in cell transwell migration (Figure 6D1 and 6D2) and phalloidin-FITC staining (Figure 6E) experiments. These data provide evidence to support the notion that NCKAP1 repression is required for miR-214–mediated inhibition of VSMC proliferation, migration, and actin polymerization.

Locally Enforced Expression of miR-214 in the Injured Arteries Inhibited NCKAP1 Expression Levels, Decreased VSMC Proliferation, and Blunted Neointima SMC Hyperplasia After Vascular Injury

To explore the functional implication of miR-214 in vascular remodeling after angioplasty, femoral arterial wire injuries were conducted, as described in our previous studies,[24,41,42] and the expression level of miR-214 was examined by RT-qPCR assay. Consistent with our in vitro findings (Figure 1), on vascular injury, the expression levels of miR-214 were substantially downregulated in femoral arteries from day 1 to 14, whereas their expression levels were almost back to normal at 28 days after angioplasty (Figure 7A), suggesting a regulatory role of miR-214 in neointima formation. To further determine the effects of miR-214 on VSMC proliferation and neointimal growth in vivo, 100 μL of 30% pluronic gel containing chemically modified and cholesterol-conjugated 2.5 nmol miR-214 or Cel-miR-67 agomirs (negative control) was applied perivascularly to femoral arteries immediately after injury, as described in our previous study.[8] Local transferring miR-214 agomirs increased vascular miR-214 levels 72 hours following wire injury to a level comparable to that of uninjured femoral artery, which was significant higher than that of injured vessels treated with Cel-miR-67 agomirs (Figure 7B). Compared with the control group, enforced expression of miR-214 in the injured vessels dramatically decreased NCKAP1 expression levels, as demonstrated in RT-qPCR (Figure 7B) and Western blotting analyses (Figure 7C and 7D). These data demonstrated an inverse correlation between miR-214 and NCKAP1 expression in the injured vessels. As expected, a decreased level of PCNA gene (Figure 7B) and protein (Figure 7C and 7D) expression was observed in the injured vessels treated with miR-214 agomirs, demonstrating that perivascular enforced expression of miR-214 in the injured vessels inhibits VSMC proliferation. Consequently, local transfection of miR-214 in the injured vessels resulted in a nearly 42% decrease in neointima formation after angioplasty (Figure 7E and 7F). As expected, a thick neointima was induced by wire injury of the femoral artery after 28 days in the mice treated with Cel-miR-67 agomirs (n=11), which significantly reduced the lumen of the vessel. However, such remodeling response was substantially inhibited by treatment with miR-214 agomirs (n=11). Our data suggest that locally restoring the expression levels of miR-214 inhibits neointima SMC hyperplasia induced by vascular injury.

Discussion

New investigations into the molecular mechanisms underlying abnormal VSMC functions and the pathogenesis of neointima

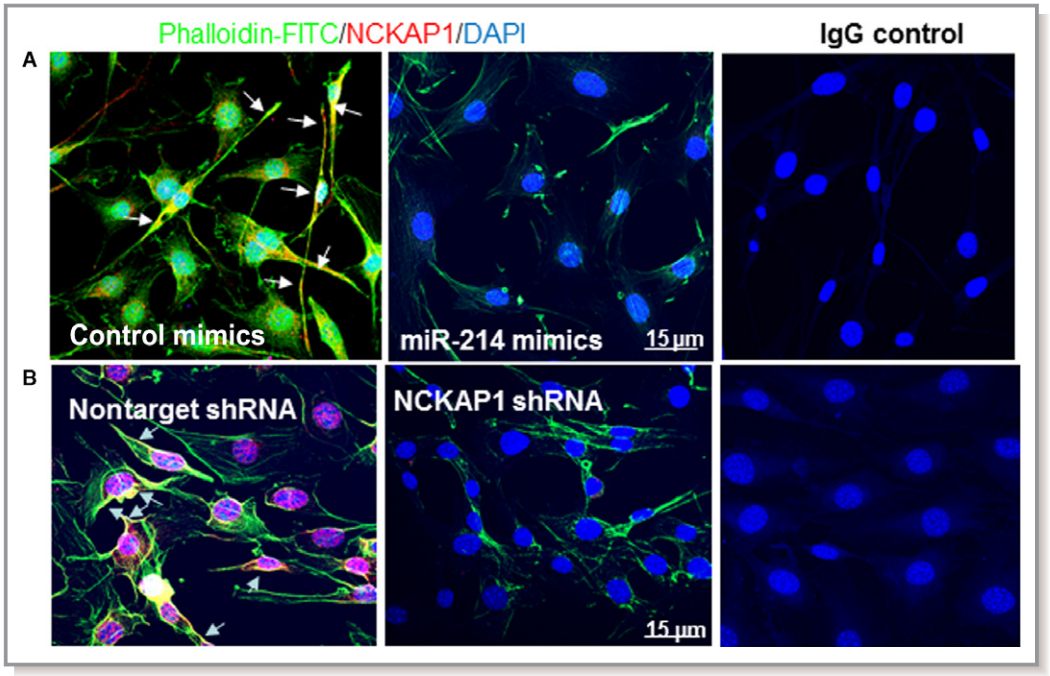

Figure 5. NCK associated protein 1 (NCKAP1) knockdown in vascular smooth muscle cells (VSMCs) recapitulates the effects of miR-214 overexpression on actin polymerization, cell migration, and proliferation. A, Actin polymerization in VSMCs was inhibited by miR-214 overexpression. VSMCs were transfected with control or miR-214 mimics, followed by serum starvation for 24 hours. Serum-starved cells were stimulated with 20% serum for another 24 hours and subjected to immunofluorescence staining with antibody against NCKAP1 and phalloidin-FITC (F-actin staining). B and C, NCKAP1 knockdown decreased actin polymerization in VSMCs. VSMCs were infected with nontarget or NCKAP1 short hairpin RNA (shRNA) virus, followed by similar treatment and analyses, as described in (A). Representative images (A and B) or mean+SEM (C) from 3 independent experiments are presented. White arrows (A and B) indicate that NCKAP1 colocalizes with F-actin within lamellipodia and membrane ruffles, which face the direction of cell movement. D through F, miR-214 overexpression or NCKAP1 knockdown inhibited VSMC proliferation (D and E) and migration (F). VSMCs were transfected with control miRNA mimics or miR-214 mimics or infected with nontarget or NCKAP1 shRNA virus, followed by serum starvation for 24 hours. Serum-starved cells were stimulated with 20% serum for another 24 hours and subjected to cell counting (D) and immunofluorescence staining with antibody against Ki-67 (E). E1, representative images; E2, quantitative data (mean+SEM) from 3 independent experiments. In another set of experiments, serum-starved cells were subjected to transwell migration assays in the presence of 30 ng/mL platelet-derived growth factor BB (F). Bar graphs show quantitative data (mean+SEM) from 3 independent experiments (n=3). **<0.01 (Compared with control mimics or nontarget shRNA). DAPI, 4′,6-diamidino-2-phenylindole; IgG, immunoglobulin G.

SMC hyperplasia are still required, and new therapeutic approaches for postangioplasty restenosis are urgently needed. In this study, we expanded our knowledge of the molecular mechanism mediating VSMC proliferation, migration, and neointima formation by uncovering an important role of miR-214 in modulating VSMC functions in vitro and in vivo. Specifically, we documented that miR-214 expression in VSMCs was modulated by different atherogenic stimuli (eg, high level of serum, PDGF-BB, 7-ketocholesterol, and 4-hydroxynonenal) and observed a decreased level of miR-214 during vascular remodeling in response to injury. Regarding cellular functions, our data showed that miR-214 regulated both VSMC proliferation and migration. Mechanistically, NCKAP1 was identified as the functional target of miR-214 in the context of VSMC functions. Moreover, our data suggested that actin polymerization and/or lamellipodia formation mediated by NCKAP1 is an underlying molecular mechanism through which miR-214 regulates VSMC growth and motility. Translationally, documented evidence suggests that locally enforced expression of miR-214 in the injured arteries can reduce NCKAP1 expression levels, inhibit VSMC proliferation, and thus blunt neointima SMC hyperplasia after vascular injury.

The miRNA miR-214 is a member of the miR-199a-214 cluster encoded by a large noncoding RNA, DNM3os, that is transcribed in the opposite strand of the *DNM3* gene.[49] Primarily, Dnm3os and the associated miR-199a-214 cluster have been suggested to play an indispensable role in normal

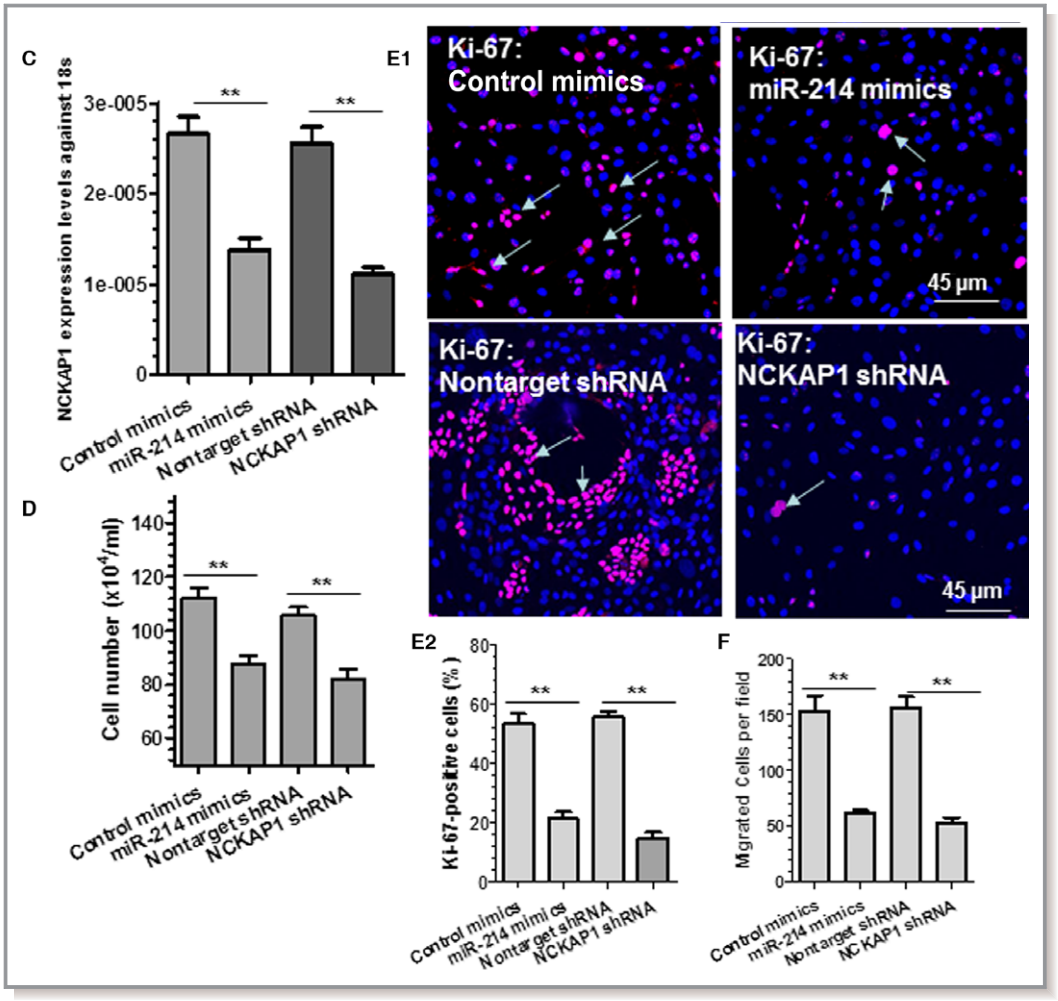

Figure 5. Continued

skeletal development and body growth in mammals,[49] probably through regulation of myogenic differentiation from precursor cells.[50] Later studies have documented a contradictory role of miR-214 in cancer progression[51,52] and cardiovascular diseases. It has been reported that genetic deletion of miR-214 in mice causes loss of cardiac contractility, increased apoptosis, and excessive fibrosis in response to ischemia–reperfusion injury, and the cardioprotective roles of miR-214 during ischemia–reperfusion injury were attributed to controlling Ca^{2+} overload and cell death.[20] This study provides evidence to support a protective role for miR-214 in protecting cardiac cells from various insults and maintaining cardiac functions. Other studies, however, proposed an opposite role for miR-214 in cardiac protection by suggesting that miR-214 provokes cardiac hypertrophy,[22] enhances the cardiac injury of viral myocarditis,[53] and mediates cardiac fibroblast proliferation and collagen synthesis.[54] The following factors likely contribute to such discrepancies: Different cell lines and animal models were used in these studies, miR-214 plays a divergent role in various cellular systems, and the functional implication of miR-214 in different biological processes depends on cell context. miR-214 has also been implicated in many other cellular functions such as promoting dendritic cell switching from tolerance to immunity,[55] regulating mitochondrial morphology and cell cycle,[56] suppressing gluconeogenesis,[57] controlling skin and hair follicle development,[58] inhibiting angiogenesis,[59–61] mediating osteogenic differentiation of myoblast cells,[62] and/or impairing mitochondrial fatty acid oxidation.[63]

Our study provides a new perspective on the role for miR-214 in VSMC biology and functions. By utilizing miRNA gain- and loss-of-function analyses, we demonstrated that miR-214 inhibits both VSMC proliferation and migration, 2 critical cellular events in vascular neointimal lesion formation, in response to higher concentration of serum or PDGF-BB, supporting a critical role of miR-214 in these VSMC functions and behaviors. Importantly, by using our well-established wire injury–induced neointima formation model and perivascular delivery of miR-214 agomirs into injured vessels, we further

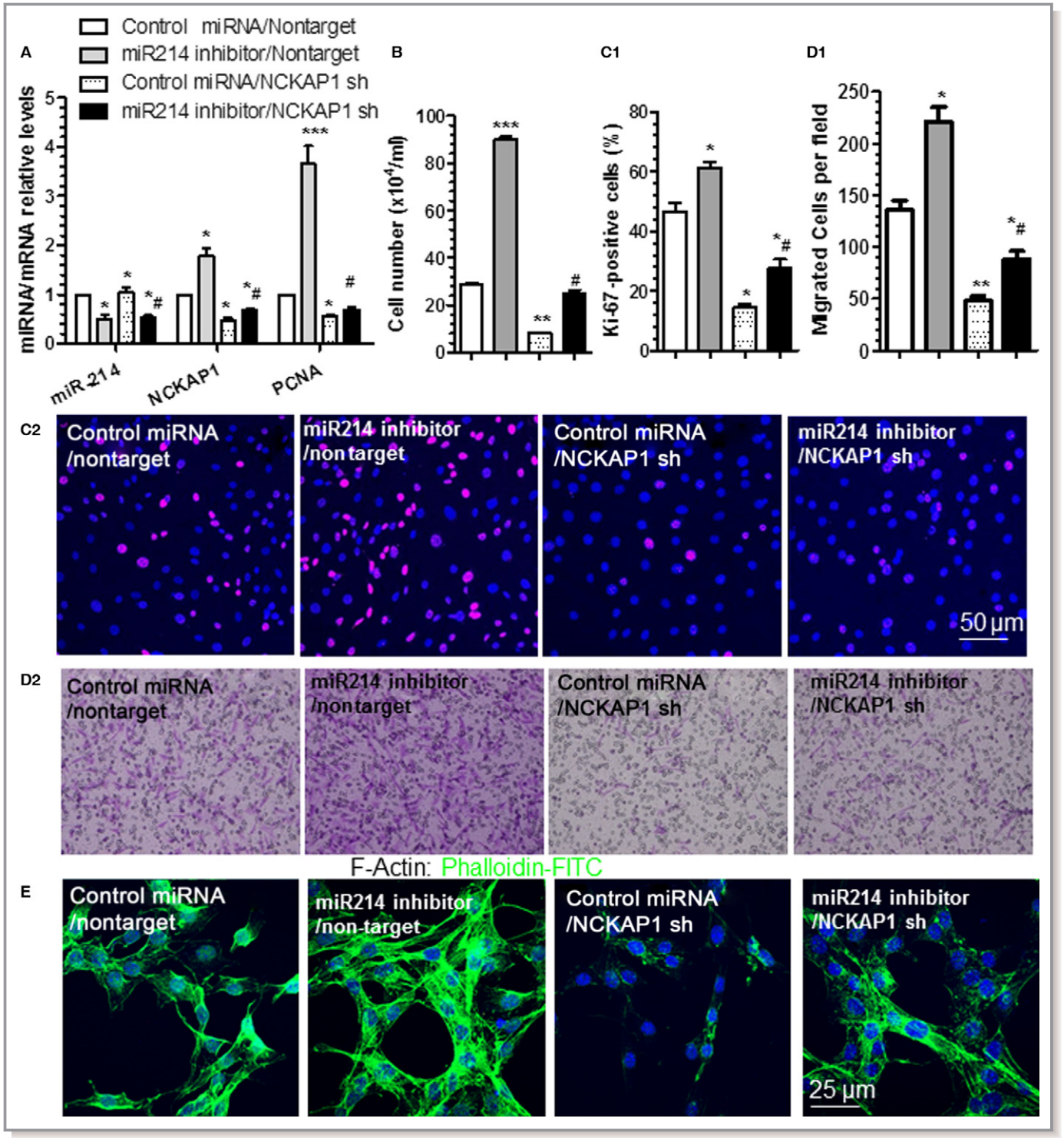

Figure 6. miR-214 mediates vascular smooth muscle cell (VSMC) growth and motility by modulating NCK associated protein 1 (NCKAP1). VSMCs were cotransduced with miR-214 inhibitor, NCKAP1 short hairpin RNA (shRNA) lentivirus (NCKAP1 sh), and/or respective controls (control microRNA [miRNA] or nontarget shRNA [nontarget]), as indicated. Transduced cells were serum-starved for 24 hours and subjected to reverse transcriptase–quantitative PCR analyses to examine miR-214, *NCKAP1*, and proliferating cell nuclear antigen (*PCNA*) expression levels (A), cell counting (B), immunofluorescence staining with antibody against Ki-67 (C1 and C2), transwell migration (D1 and D2), and F-actin staining using phalloidin-FITC (E) in response to serum (A through C and E) or 30 ng/mL platelet-derived growth factor BB (D) stimulation. The data presented are representative images (C2, D2 and E) or mean+SEM (A, B, C1 and D1) of 3 independent experiments. *<0.05, **<0.01, ***<0.001 (Compared various treatments with double control), #<0.05 (Compared NCKAP1 knockdown with control in VSMCs with miR-214 inhibition).

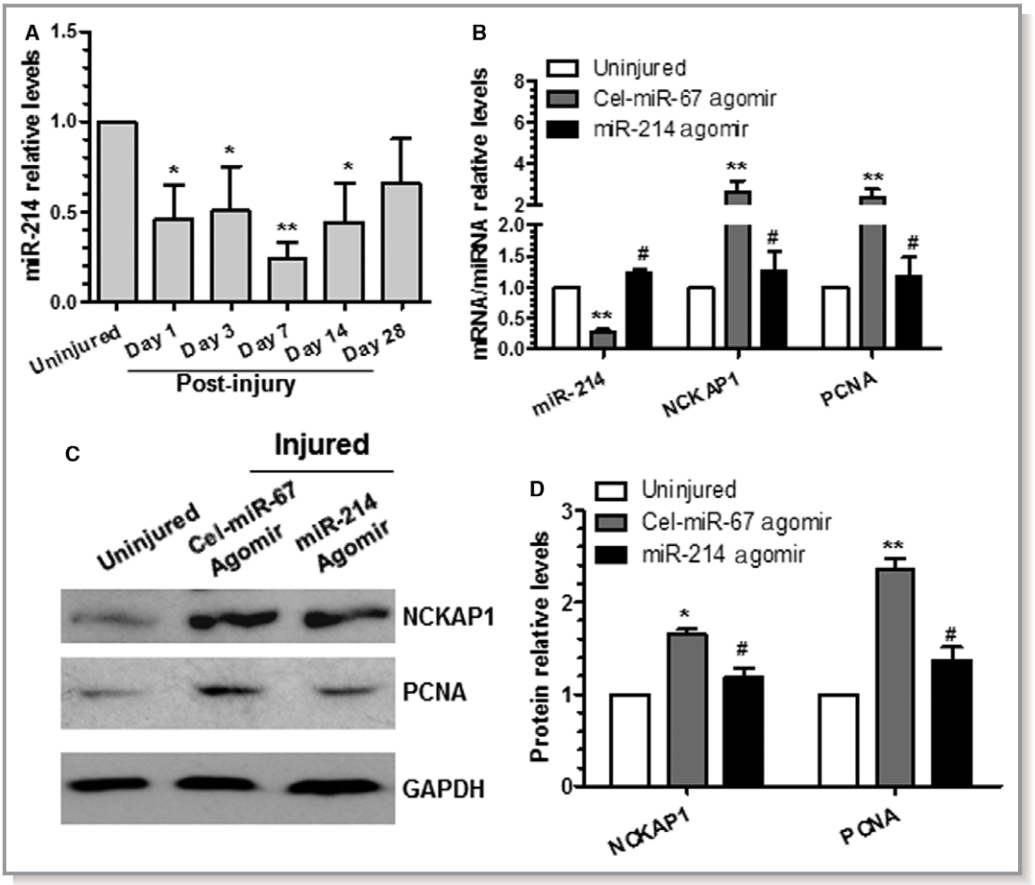

Figure 7. Locally enforced expression of miR-214 in the injured arteries inhibited NCK associated protein 1 (NCKAP1) expression levels, decreased smooth muscle cell proliferation, and blunted neointima hyperplasia after vascular injury. A, miR-214 was downregulated after injury. *<0.05, **<0.01 (Compared with uninjured control). B through D, Gene/protein expression levels in the injured vessels were modulated by perivascular delivery of miR-214 agomirs. After injury, 100 μL of 30% pluronic gel containing 2.5 nmol agomirs per vessel per mouse was immediately applied and packed around the injured vessel. At 3 days (B), 14 days (C and D), or 28 days (E and F) later, injured segments of femoral arteries were harvested and subjected to various studies, as indicated. Total RNAs and proteins were extracted from uninjured and injured vessels (femoral arteries from 3 to 5 mice were pooled for each experiment, n=3 experiments) and subjected to reverse transcriptase–quantitative PCR (B) and Western blotting (C and D) analyses. Representative images (C) and quantitative data (mean+SEM) (B and D) of 3 independent experiments are presented. E and F, Wire injury–induced neointima formation was blunted by miR-214 overexpression. Paraffin sections from both groups (n=11 mice for each group) were prepared and subjected to hematoxylin and eosin staining analyses. Representative images (E) and quantitative morphological characteristics (mean+SEM) including media area, neointimal area, neointimal/media ratio, and lumen area (F) are presented. #<0.05 (Compared miR-214 agomirs with Cel-miR-67 agomirs [B, D and F]). *<0.05, **<0.01 (Compared with uninjured vessels [B and D]).

demonstrated that miR-214 modulated VSMC proliferation and inhibited neointima SMC hyperplasia, suggesting that miR-214 is a potential therapeutic agent in postangioplasty restenosis. Consequently, findings from this study and previous studies indicate that miR-214 exerts a divergent role in various cellular functions and a wide range of human diseases (particularly cancers and cardiovascular diseases), and more caution should be taken when considering the therapeutic effects of miR-214 overexpression and/or inhibition on distinct human diseases.

A new finding in this study is that miR-214 can be modulated by different atherogenic stimuli (eg, high level of serum, PDGF-BB, 7-ketocholesterol, and 4-hydroxynonenal) in both human and murine VSMCs. miR-214 is upregulated in response to several factors including cardiac stress, myocardial infarction, Ca^{2+} overload,[18,19] and heart failure.[59] It has been reported that miR-214 is hypoxia-inducible miRNA and can be regulated in a HIF1α-dependent and/or HIF1α-independent manner.[63] It is currently unknown whether the abovementioned atherogenic stimuli downregulate miR-214

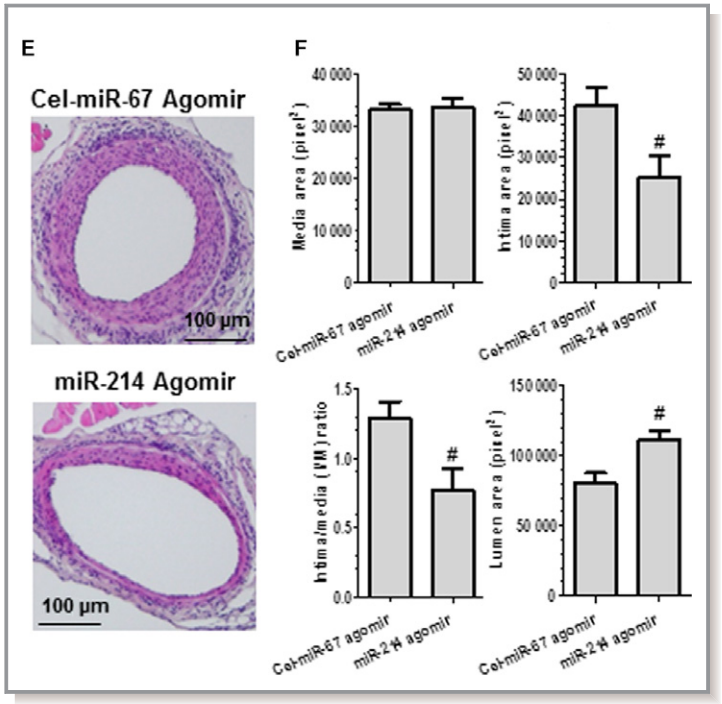

Figure 7. Continued

expression in VSMCs through an HIF1α-dependent and/or HIF1α-independent mechanism; however, it is unlikely that the HIF1α signaling pathway will be involved in miR-214 modulation by atherogenic stimuli because the VSMCs were cultured under normoxic but not hypoxic conditions in this study. Instead, our data (Figure 1D through 1H) demonstrated that both serum and PDGF-BB regulate miR-214 expression through a transcriptional mechanism, an E-box element within the miR-214 promoter, that can be bound by the basic helix-loop-helix transcription factor Twist-1, which is required for such regulation, and that both atherogenic stimuli can downregulate Twist-1 gene expression in VSMCs. Our data are consistent with the previous finding that miR-214 expression in hepatic stellate cells[64] and during development[34] is dependent on Twist-1.

Another major novel finding in this study is that we identified *NCKAP1* as the functional target gene of miR-214 in VSMC functions and related diseases. Although multiple miR-214 targets have been reported in various cellular contexts and diseases (eg, ITCH,[53] TFAP2C,[52] Osterix,[62] FGFR1,[51] PPARδ,[63] Quaking,[60] Ncx1,[20] β-catenin,[55,58] Mitofusin2,[56] and ATF4[57]), we provided evidence to suggest that *NCKAP1* is a novel target gene of miR-214 in VSMCs (Figure 4 and Figure S1) and is required for miR-214 mediation of VSMC growth and migration (Figures 5 and 6). Cell migration is a highly orchestrated multistep process. It has been elegantly proposed that in response to extracellular signals, a cell initially extends its flat membrane protrusions (lamellipodia) and fingerlike protrusions (filopodia) and forms adhesions at the cell front (or leading edge), followed by retracting its tail to move forward.[65] The actin cytoskeleton and associated proteins play a major role in this process. NCKAP1 (or p125Nap1) was primarily shown to associate with NCK (noncatalytic region of tyrosine kinase adaptor protein 1) both in vitro and in intact cells through binding to the Src homology 3 (SH3) domains of NCK[66] and was found to localize along the lamellipodia and to mediate contact-dependent cell migration.[67] A later study also suggested a critical developmental role for NCKAP1 because mice lacking this gene will be arrested at midgestation and have defects in morphogenesis of all 3 embryonic germ layers.[68] Unsurprisingly, as a constitutive and essential component of a WAVE complex, NCKAP1 has been reported to play a key role in regulation of cell motility and adhesion by driving actin assembly and polymerization and lamellipodia formation.[48,69] Nevertheless, the mechanism through which NCKAP1 is modulated in the context of VSMC functions remains elusive. In the current study, we demonstrated for the first time that NCKAP1 is regulated by miR-214 in VSMCs. In our proteomics analyses, NCKAP1 was found to be one of the top downregulated proteins with the highest confidence and significance (Figure 4B). Importantly, 3 miR-214 binding sites were found within the 3′UTR of *NCKAP1*, all of them with favorable minimum loop-free energy in the formation of the miR-214: *NCKAP1* 3′UTR duplex stem loop (Figure S1). Moreover, our data showed that NCKAP1 is reversely regulated by miR-214 in VSMCs because miR-214 overexpression significantly downregulated, whereas miR-214 inhibition increased,

NCKAP1 expression (Figure 4). Luciferase reporter and mutagenesis assays finally confirmed that NCKAP1 is the direct and functional target of miR-214.

Functionally and mechanistically, we also demonstrated that controlling actin assembly and polymerization and lamellipodia formation in VSMCs through modulation of NCKAP1 expression is a primary mechanism through which miR-214 mediates VSMC functions and behaviors including growth and movement. We observed a much lower level of F-actin and lamellipodia formation and a significantly decreased level of NCKAP1 in miR-214–overexpressing VSMCs (Figure 5A), suggesting that miR-214 impairs actin assembly and polymerization and lamellipodia formation through inhibition of NCKAP1. Additional data from NCKAP1 knockdown experiments (Figure 5B through 5F) showed that NCKAP1 inhibition can recapitulate the inhibitory effects of miR-214 overexpression on VSMC functions and behaviors. Finally, evidence from the cotransduction experiments (miR-214 inhibition and NCKAP1 knockdown) (Figure 6) indicated that NCKAP1 repression is required for miR-214–mediated inhibition of VSMC proliferation, migration, and actin polymerization. Consistently, our data showed that NCKAP1 is colocalized with F-actin within lamellipodia at the cell front (Figure 5A and 5B); however, we unexpectedly observed that NCKAP1 can be relocalized inside the nuclei of VSMCs, particularly after the cells were subjected to serum-starvation treatment (Figure 5B). The functional implication of such unexpected findings warrants further investigation in a separate study. Moreover, we observed a higher level of nuclear localization of NCKAP1 in control VSMCs infected with shRNA lentivirus (Figure 5B) than in VSMCs transfected with control miRNA mimics (Figure 5A). Because these 2 control VSMCs were subjected to different treatments (cells with control miRNA mimics received transient transfection for 24 hours, whereas the control VSMCs with nontarget shRNA were generated from lentivirus infection and a 10-day puromycin selection) prior to serum starvation, we speculated that such discrepancies were due to the additive or synergistic effects of serum restimulation and lentivirus infection (and/or puromycin selection during cell line generation), which is under investigation in our separate study.

Apart from NCKAP1, which was identified and validated as a bona fide miR-214 mRNA target in VSMCs in the current study, the abovementioned studies also suggest that multiple other genes can be regulated by miR-214 in other cellular contexts and related diseases. Interestingly, only 2 reported miR-214 targets—β-catenin[55,58] and PCBP2[70]—were slightly repressed by miR-214 in VSMCs, as demonstrated in our proteomics analyses (Table S2). All other reported miR-214 target genes failed to pass the threshold setting for our proteomics analyses, likely because VSMCs contain lower amounts or lack of expression of these target proteins or because of low sensitivity in identifying such regulatory proteins in the whole-cell lysate using proteomics analyses. Despite this limitation, data from our proteomics analysis showed that the majority of the proteins downregulated by miR-214 are involved in regulation of cell migration, actin filament reorganization and actin polymerization, proliferation, cell cycle, and gene expression, further supporting a role of miR-214 in VSMC proliferation and migration. The fact that multiple genes were identified as the functional targets of miR-214 in different studies suggests that miR-214 plays a divergent role under various physiological and pathological conditions by targeting distinct target genes and/or that miR-214 regulates its target genes in a cellular context–dependent manner.

Surprisingly, our proteomics data showed that more proteins were upregulated in VSMCs by miR-214 (160 and 59 for upregulated and downregulated proteins, respectively) (Table S2), which suggests that miR-214 positively regulates these proteins by suppressing ≥1 major transcription/epigenetic factor. Indeed, we observed that SMYD5, an epigenetic regulator, was significantly downregulated by miR-214 overexpression. Moreover, data from reporter luciferase assays showed that miR-214 overexpression significantly repressed *SMYD5* 3′UTR reporter activity (Figure S2B), providing direct evidence to support *SMYD5* as a target gene of miR-214 in VSMCs. SMYD5 belongs to the class V–like SAM-binding methyltransferase superfamily, which has been suggested to play an important role in regulation of gene silencing by modulating the methylation of a variety of histone and nonhistone targets.[71] It would be plausible that miR-214 could upregulate a large number of proteins in VSMCs by desuppressing SMYD5; however, the implications of modulated SMYD5 in VSMC functions remain to be further investigated.

It is worth mentioning that in response to injury, lack of reendothelialization represents another major contribution to neointimal formation. Several studies[59–61] have suggested that miR-214 may play a role in regulating angiogenesis; therefore, the biological effects of miR-214 on endothelial cells and reendothelialization after injury may also contribute to the miR-214–mediated effect on vascular remodeling and needs to be investigated in future studies. Nonetheless, in the current study, we successfully uncovered the functional involvements of miR-214 in VSMC biology and in vascular remodeling after injury. Moreover, the newly identified target NCKAP1 is at least partially responsible for miR-214–mediated VSMC functions. Taken together, the findings presented in the current study suggest that modulated miR-214 can be a potential therapeutic target for VSMC-related diseases such as atherosclerosis and postangioplasty restenosis.

Sources of Funding

This work was supported by British Heart Foundation (FS/09/044/28007, PG/11/40/28891, PG/13/45/30326, PG/15/11/31279, PG/15/86/31723 and PG/16/1/31892 to Xiao); National Natural Science Foundation of China Grant (91339102, 30900571, 81270001, 81570249, 91539103, and 81270180); and Zhejiang Provincial Nature Science Foundation (LR14H020001). This work forms part of the research themes contributing to the translational research portfolio of Barts and the London Cardiovascular Biomedical Research Unit which is supported and funded by the National Institute of Health Research.

Disclosures

None.

References

1. Johnson JL. Emerging regulators of vascular smooth muscle cell function in the development and progression of atherosclerosis. *Cardiovasc Res*. 2014;103:452–460.
2. Ambros V. The functions of animal microRNAs. *Nature*. 2004;431:350–355.
3. Albinsson S, Suarez Y, Skoura A, Offermanns S, Miano JM, Sessa WC. MicroRNAs are necessary for vascular smooth muscle growth, differentiation, and function. *Arterioscler Thromb Vasc Biol*. 2010;30:1118–1126.
4. Bonauer A, Boon RA, Dimmeler S. Vascular microRNAs. *Curr Drug Targets*. 2010;11:943–949.
5. Chen J, Yin H, Jiang Y, Radhakrishnan SK, Huang ZP, Li J, Shi Z, Kilsdonk EP, Gui Y, Wang DZ, Zheng XL. Induction of microRNA-1 by myocardin in smooth muscle cells inhibits cell proliferation. *Arterioscler Thromb Vasc Biol*. 2011;31:368–375.
6. Ji R, Cheng Y, Yue J, Yang J, Liu X, Chen H, Dean DB, Zhang C. MicroRNA expression signature and antisense-mediated depletion reveal an essential role of microRNA in vascular neointimal lesion formation. *Circ Res*. 2007;100:1579–1588.
7. Wang M, Li W, Chang GQ, Ye CS, Ou JS, Li XX, Liu Y, Cheang TY, Huang XL, Wang SM. MicroRNA-21 regulates vascular smooth muscle cell function via targeting tropomyosin 1 in arteriosclerosis obliterans of lower extremities. *Arterioscler Thromb Vasc Biol*. 2011;31:2044–2053.
8. Chen Q, Yang F, Guo M, Wen G, Zhang C, Luong le A, Zhu J, Xiao Q, Zhang L. miRNA-34a reduces neointima formation through inhibiting smooth muscle cell proliferation and migration. *J Mol Cell Cardiol*. 2015;89:75–86.
9. Torella D, Iaconetti C, Catalucci D, Ellison GM, Leone A, Waring CD, Bochicchio A, Vicinanza C, Aquila I, Curcio A, Condorelli G, Indolfi C. MicroRNA-133 controls vascular smooth muscle cell phenotypic switch in vitro and vascular remodeling in vivo. *Circ Res*. 2011;109:880–893.
10. Liu X, Cheng Y, Zhang S, Lin Y, Yang J, Zhang C. A necessary role of miR-221 and miR-222 in vascular smooth muscle cell proliferation and neointimal hyperplasia. *Circ Res*. 2009;104:476–487.
11. Davis BN, Hilyard AC, Nguyen PH, Lagna G, Hata A. Induction of microRNA-221 by platelet-derived growth factor signaling is critical for modulation of vascular smooth muscle phenotype. *J Biol Chem*. 2009;284:3728–3738.
12. Boettger T, Beetz N, Kostin S, Schneider J, Kruger M, Hein L, Braun T. Acquisition of the contractile phenotype by murine arterial smooth muscle cells depends on the Mir143/145 gene cluster. *J Clin Invest*. 2009;119:2634–2647.
13. Cheng Y, Liu X, Yang J, Lin Y, Xu DZ, Lu Q, Deitch EA, Huo Y, Delphin ES, Zhang C. MicroRNA-145, a novel smooth muscle cell phenotypic marker and modulator, controls vascular neointimal lesion formation. *Circ Res*. 2009;105:158–166.
14. Zhao N, Koenig SN, Trask AJ, Lin CH, Hans CP, Garg V, Lilly B. MicroRNA miR145 regulates TGFBR2 expression and matrix synthesis in vascular smooth muscle cells. *Circ Res*. 2015;116:23–34.
15. Elia L, Quintavalle M, Zhang J, Contu R, Cossu L, Latronico MV, Peterson KL, Indolfi C, Catalucci D, Chen J, Courtneidge SA, Condorelli G. The knockout of miR-143 and -145 alters smooth muscle cell maintenance and vascular homeostasis in mice: correlates with human disease. *Cell Death Differ*. 2009;16:1590–1598.
16. Li P, Liu Y, Yi B, Wang G, You X, Zhao X, Summer R, Qin Y, Sun J. MicroRNA-638 is highly expressed in human vascular smooth muscle cells and inhibits PDGF-BB-induced cell proliferation and migration through targeting orphan nuclear receptor NOR1. *Cardiovasc Res*. 2013;99:185–193.
17. Li P, Zhu N, Yi B, Wang N, Chen M, You X, Zhao X, Solomides CC, Qin Y, Sun J. MicroRNA-663 regulates human vascular smooth muscle cell phenotypic switch and vascular neointimal formation. *Circ Res*. 2013;113:1117–1127.
18. van Rooij E, Sutherland LB, Liu N, Williams AH, McAnally J, Gerard RD, Richardson JA, Olson EN. A signature pattern of stress-responsive microRNAs that can evoke cardiac hypertrophy and heart failure. *Proc Natl Acad Sci USA*. 2006;103:18255–18260.
19. van Rooij E, Sutherland LB, Thatcher JE, DiMaio JM, Naseem RH, Marshall WS, Hill JA, Olson EN. Dysregulation of microRNAs after myocardial infarction reveals a role of miR-29 in cardiac fibrosis. *Proc Natl Acad Sci USA*. 2008;105:13027–13032.
20. Aurora AB, Mahmoud AI, Luo X, Johnson BA, van Rooij E, Matsuzaki S, Humphries KM, Hill JA, Bassel-Duby R, Sadek HA, Olson EN. MicroRNA-214 protects the mouse heart from ischemic injury by controlling Ca^{2+} overload and cell death. *J Clin Invest*. 2012;122:1222–1232.
21. Lu HQ, Liang C, He ZQ, Fan M, Wu ZG. Circulating miR-214 is associated with the severity of coronary artery disease. *J Geriatr Cardiol*. 2013;10:34–38.
22. Yang T, Zhang GF, Chen XF, Gu HH, Fu SZ, Xu HF, Feng Q, Ni YM. MicroRNA-214 provokes cardiac hypertrophy via repression of EZH2. *Biochem Biophys Res Commun*. 2013;436:578–584.
23. Yu X, Zhang L, Wen G, Zhao H, Luong LA, Chen Q, Huang Y, Zhu J, Ye S, Xu Q, Wang W, Xiao Q. Upregulated sirtuin 1 by miRNA-34a is required for smooth muscle cell differentiation from pluripotent stem cells. *Cell Death Differ*. 2015;22:1170–1180.
24. Xiao Q, Zhang F, Grassia G, Hu Y, Zhang Z, Xing Q, Yin X, Maddaluno M, Drung B, Schmidt B, Maffia P, Ialenti A, Mayr M, Xu Q, Ye S. Matrix metalloproteinase-8 promotes vascular smooth muscle cell proliferation and neointima formation. *Arterioscler Thromb Vasc Biol*. 2014;34:90–98.
25. Wang L, Zheng J, Du Y, Huang Y, Li J, Liu B, Liu CJ, Zhu Y, Gao Y, Xu Q, Kong W, Wang X. Cartilage oligomeric matrix protein maintains the contractile phenotype of vascular smooth muscle cells by interacting with alpha(7)beta (1) integrin. *Circ Res*. 2010;106:514–525.
26. Salmon M, Gomez D, Greene E, Shankman L, Owens GK. Cooperative binding of KLF4, pELK-1, and HDAC2 to a G/C repressor element in the SM22α promoter mediates transcriptional silencing during SMC phenotypic switching in vivo. *Circ Res*. 2012;111:685–696.
27. Chahine MN, Blackwood DP, Dibrov E, Richard MN, Pierce GN. Oxidized LDL affects smooth muscle cell growth through MAPK-mediated actions on nuclear protein import. *J Mol Cell Cardiol*. 2009;46:431–441.
28. Auge N, Garcia V, Maupas-Schwalm F, Levade T, Salvayre R, Negre-Salvayre A. Oxidized LDL-induced smooth muscle cell proliferation involves the EGF receptor/PI-3 kinase/Akt and the sphingolipid signaling pathways. *Arterioscler Thromb Vasc Biol*. 2002;22:1990–1995.
29. Zhao H, Wen G, Huang Y, Yu X, Chen Q, Afzal TA, Luong le A, Zhu J, Ye S, Zhang L, Xiao Q. MicroRNA-22 regulates smooth muscle cell differentiation from stem cells by targeting methyl CpG-binding protein 2. *Arterioscler Thromb Vasc Biol*. 2015;35:918–929.
30. Luo Z, Wen G, Wang G, Pu X, Ye S, Xu Q, Wang W, Xiao Q. MicroRNA-200C and -150 play an important role in endothelial cell differentiation and vasculogenesis by targeting transcription repressor ZEB1. *Stem Cells*. 2013;31:1749–1762.
31. Xiao Q, Zhang F, Lin L, Fang C, Wen G, Tsai TN, Pu X, Sims D, Zhang Z, Yin X, Thomaszewski B, Schmidt B, Mayr M, Suzuki K, Xu Q, Ye S. Functional role of matrix metalloproteinase-8 in stem/progenitor cell migration and their recruitment into atherosclerotic lesions. *Circ Res*. 2013;112:35–47.
32. Huang Y, Lin L, Yu X, Wen G, Pu X, Zhao H, Fang C, Zhu J, Ye S, Zhang L, Xiao Q. Functional involvements of heterogeneous nuclear ribonucleoprotein A1 in smooth muscle differentiation from stem cells in vitro and in vivo. *Stem Cells*. 2013;31:906–917.
33. Fang C, Wen G, Zhang L, Lin L, Moore A, Wu S, Ye S, Xiao Q. An important role of matrix metalloproteinase-8 in angiogenesis in vitro and in vivo. *Cardiovasc Res*. 2013;99:146–155.
34. Lee YB, Bantounas I, Lee DY, Phylactou L, Caldwell MA, Uney JB. Twist-1 regulates the miR-199a/214 cluster during development. *Nucleic Acids Res*. 2009;37:123–128.
35. Liang CC, Park AY, Guan JL. In vitro scratch assay: a convenient and inexpensive method for analysis of cell migration in vitro. *Nat Protoc*. 2007;2:329–333.

36. Wen G, Zhang C, Chen Q, le Luong A, Mustafa A, Ye S, Xiao Q. A novel role of matrix metalloproteinase-8 in macrophage differentiation and polarization. *J Biol Chem*. 2015;290:19158–19172.
37. Alcolea MP, Casado P, Rodriguez-Prados JC, Vanhaesebroeck B, Cutillas PR. Phosphoproteomic analysis of leukemia cells under basal and drug-treated conditions identifies markers of kinase pathway activation and mechanisms of resistance. *Mol Cell Proteomics*. 2012;11:453–466.
38. Montoya A, Beltran L, Casado P, Rodriguez-Prados JC, Cutillas PR. Characterization of a TiO(2) enrichment method for label-free quantitative phosphoproteomics. *Methods*. 2011;54:370–378.
39. Rajeeve V, Vendrell I, Wilkes E, Torbett N, Cutillas PR. Cross-species proteomics reveals specific modulation of signaling in cancer and stromal cells by phosphoinositide 3-kinase (PI3K) inhibitors. *Mol Cell Proteomics*. 2014;13:1457–1470.
40. Cutillas PR, Vanhaesebroeck B. Quantitative profile of five murine core proteomes using label-free functional proteomics. *Mol Cell Proteomics*. 2007;6:1560–1573.
41. Xiao Q, Zeng L, Zhang Z, Margariti A, Ali ZA, Channon KM, Xu Q, Hu Y. Sca-1+ progenitors derived from embryonic stem cells differentiate into endothelial cells capable of vascular repair after arterial injury. *Arterioscler Thromb Vasc Biol*. 2006;26:2244–2251.
42. Zeng L, Xiao Q, Margariti A, Zhang Z, Zampetaki A, Patel S, Capogrossi MC, Hu Y, Xu Q. HDAC3 is crucial in shear- and VEGF-induced stem cell differentiation toward endothelial cells. *J Cell Biol*. 2006;174:1059–1069.
43. Cai J, Yang C, Yang Q, Ding H, Jia J, Guo J, Wang J, Wang Z. Deregulation of let-7e in epithelial ovarian cancer promotes the development of resistance to cisplatin. *Oncogenesis*. 2013;2:e75.
44. Wang X, Guo B, Li Q, Peng J, Yang Z, Wang A, Li D, Hou Z, Lv K, Kan G, Cao H, Wu H, Song J, Pan X, Sun Q, Ling S, Li Y, Zhu M, Zhang P, Peng S, Xie X, Tang T, Hong A, Bian Z, Bai Y, Lu A, He F, Zhang G. miR-214 targets ATF4 to inhibit bone formation. *Nat Med*. 2013;19:93–100.
45. Krutzfeldt J, Rajewsky N, Braich R, Rajeev KG, Tuschl T, Manoharan M, Stoffel M. Silencing of microRNAs in vivo with 'antagomirs'. *Nature*. 2005;438:685–689.
46. Trajkovski M, Hausser J, Soutschek J, Bhat B, Akin A, Zavolan M, Heim MH, Stoffel M. MicroRNAs 103 and 107 regulate insulin sensitivity. *Nature*. 2011;474:649–653.
47. Pidkovka NA, Cherepanova OA, Yoshida T, Alexander MR, Deaton RA, Thomas JA, Leitinger N, Owens GK. Oxidized phospholipids induce phenotypic switching of vascular smooth muscle cells in vivo and in vitro. *Circ Res*. 2007;101:792–801.
48. Steffen A, Rottner K, Ehinger J, Innocenti M, Scita G, Wehland J, Stradal TE. Sra-1 and Nap1 link Rac to actin assembly driving lamellipodia formation. *EMBO J*. 2004;23:749–759.
49. Watanabe T, Sato T, Amano T, Kawamura Y, Kawamura N, Kawaguchi H, Yamashita N, Kurihara H, Nakaoka T. Dnm3os, a non-coding RNA, is required for normal growth and skeletal development in mice. *Dev Dyn*. 2008;237:3738–3748.
50. Liu J, Luo XJ, Xiong AW, Zhang ZD, Yue S, Zhu MS, Cheng SY. MicroRNA-214 promotes myogenic differentiation by facilitating exit from mitosis via down-regulation of proto-oncogene N-ras. *J Biol Chem*. 2010;285:26599–26607.
51. Chen DL, Wang ZQ, Zeng ZL, Wu WJ, Zhang DS, Luo HY, Wang F, Qiu MZ, Wang DS, Ren C, Wang FH, Chiao LJ, Pelicano H, Huang P, Li YH, Xu RH. Identification of microRNA-214 as a negative regulator of colorectal cancer liver metastasis by way of regulation of fibroblast growth factor receptor 1 expression. *Hepatology*. 2014;60:598–609.
52. Penna E, Orso F, Cimino D, Tenaglia E, Lembo A, Quaglino E, Poliseno L, Haimovic A, Osella-Abate S, De Pitta C, Pinatel E, Stadler MB, Provero P, Bernengo MG, Osman I, Taverna D. MicroRNA-214 contributes to melanoma tumour progression through suppression of TFAP2C. *EMBO J*. 2011;30:1990–2007.
53. Chen ZG, Liu H, Zhang JB, Zhang SL, Zhao LH, Liang WQ. Upregulated microRNA-214 enhances cardiac injury by targeting ITCH during coxsackievirus infection. *Mol Med Rep*. 2015;12:1258–1264.
54. Sun M, Yu H, Zhang Y, Li Z, Gao W. MicroRNA-214 mediates isoproterenol-induced proliferation and collagen synthesis in cardiac fibroblasts. *Sci Rep*. 2015;5:18351.
55. Gu C, Zhou XD, Yuan Y, Miao XH, Liu Y, Ru YW, Li KQ, Li G. MicroRNA-214 induces dendritic cell switching from tolerance to immunity by targeting beta-catenin signaling. *Int J Clin Exp Pathol*. 2015;8:10050–10060.
56. Bucha S, Mukhopadhyay D, Bhattacharyya NP. Regulation of mitochondrial morphology and cell cycle by microRNA-214 targeting Mitofusin2. *Biochem Biophys Res Commun*. 2015;465:797–802.
57. Li K, Zhang J, Yu J, Liu B, Guo Y, Deng J, Chen S, Wang C, Guo F. MicroRNA-214 suppresses gluconeogenesis by targeting activating transcriptional factor 4. *J Biol Chem*. 2015;290:8185–8195.
58. Ahmed MI, Alam M, Emelianov VU, Poterlowicz K, Patel A, Sharov AA, Mardaryev AN, Botchkareva NV. MicroRNA-214 controls skin and hair follicle development by modulating the activity of the Wnt pathway. *J Cell Biol*. 2014;207:549–567.
59. Duan Q, Yang L, Gong W, Chaugai S, Wang F, Chen C, Wang P, Zou MH, Wang DW. MicroRNA-214 is upregulated in heart failure patients and suppresses XBP1-mediated endothelial cells angiogenesis. *J Cell Physiol*. 2015;230:1964–1973.
60. van Mil A, Grundmann S, Goumans MJ, Lei Z, Oerlemans MI, Jaksani S, Doevendans PA, Sluijter JP. MicroRNA-214 inhibits angiogenesis by targeting quaking and reducing angiogenic growth factor release. *Cardiovasc Res*. 2012;93:655–665.
61. Chan LS, Yue PY, Mak NK, Wong RN. Role of microRNA-214 in ginsenoside-Rg1-induced angiogenesis. *Eur J Pharm Sci*. 2009;38:370–377.
62. Shi K, Lu J, Zhao Y, Wang L, Li J, Qi B, Li H, Ma C. MicroRNA-214 suppresses osteogenic differentiation of C2C12 myoblast cells by targeting Osterix. *Bone*. 2013;55:487–494.
63. el Azzouzi H, Leptidis S, Dirkx E, Hoeks J, van Bree B, Brand K, McClellan EA, Poels E, Sluimer JC, van den Hoogenhof MM, Armand AS, Yin X, Langley S, Bourajjaj M, Olieslagers S, Krishnan J, Vooijs M, Kurihara H, Stubbs A, Pinto YM, Krek W, Mayr M, da Costa Martins PA, Schrauwen P, De Windt LJ. The hypoxia-inducible microRNA cluster miR-199a approximately 214 targets myocardial PPARδ and impairs mitochondrial fatty acid oxidation. *Cell Metab*. 2013;18:341–354.
64. Chen L, Chen R, Kemper S, Charrier A, Brigstock DR. Suppression of fibrogenic signaling in hepatic stellate cells by Twist1-dependent microRNA-214 expression: role of exosomes in horizontal transfer of Twist1. *Am J Physiol Gastrointest Liver Physiol*. 2015;309:G491–G499.
65. Le Clainche C, Carlier MF. Regulation of actin assembly associated with protrusion and adhesion in cell migration. *Physiol Rev*. 2008;88:489–513.
66. Kitamura T, Kitamura Y, Yonezawa K, Totty NF, Gout I, Hara K, Waterfield MD, Sakaue M, Ogawa W, Kasuga M. Molecular cloning of p125Nap1, a protein that associates with an SH3 domain of Nck. *Biochem Biophys Res Commun*. 1996;219:509–514.
67. Nakao S, Platek A, Hirano S, Takeichi M. Contact-dependent promotion of cell migration by the OL-protocadherin-Nap1 interaction. *J Cell Biol*. 2008;182:395–410.
68. Rakeman AS, Anderson KV. Axis specification and morphogenesis in the mouse embryo require Nap1, a regulator of WAVE-mediated actin branching. *Development*. 2006;133:3075–3083.
69. Ibarra N, Blagg SL, Vazquez F, Insall RH. Nap1 regulates Dictyostelium cell motility and adhesion through SCAR-dependent and -independent pathways. *Curr Biol*. 2006;16:717–722.
70. Tang SL, Gao YL, Chen XB. MicroRNA-214 targets PCBP2 to suppress the proliferation and growth of glioma cells. *Int J Clin Exp Pathol*. 2015;8:12571–12576.
71. Spellmon N, Holcomb J, Trescott L, Sirinupong N, Yang Z. Structure and function of SET and MYND domain-containing proteins. *Int J Mol Sci*. 2015;16:1406–1428.

JAHA/2016/004629-T1R1

SUPPLEMENTARY DATA

NCKAP1 Modulated by miRNA-214 Determines Vascular Smooth Muscle Cell Migration, Proliferation and Neointima Hyperplasia

Tayyab Adeel Afzal[1#], Le Anh Luong[1#], Dan Chen[1,2], Cheng Zhang[1,2], Feng Yang[1,3], Qishan Chen[1,3], Weiwei An[1], Edmund Wilkes[5], Kenta Yashiro[4], Pedro R. Cutillas[5], Li Zhang[3*] and Qingzhong Xiao[1*]

[1]Centre for Clinical Pharmacology and [4]Translational Medicine & Therapeutics, William Harvey Research Institute, Barts and The London School of Medicine and Dentistry, Queen Mary University of London, London EC1M 6BQ, UK;
[2]Department of Cardiothoracic Surgery, The First Affiliated Hospital of Chongqing Medical University, 400016, Chongqing, China;
[3]Department of Cardiology, the First Affiliated Hospital, School of Medicine, Zhejiang University, 79 Qingchun Road, Hangzhou, 310003, Zhejiang, China;
[5]Centre for Haemato-Oncology, Barts Cancer Institute, Barts and The London School of Medicine and Dentistry, Queen Mary University of London, London EC1M 6BQ, UK.

[#]T Afzal and L Luong contributed equally to this study

*Correspondence to:
Dr Qingzhong Xiao (q.xiao@qmul.ac.uk***)***, Centre for Clinical Pharmacology, William Harvey Research Institute, Barts and The London School of Medicine and Dentistry, Queen Mary University of London, Heart Centre, Charterhouse Square, London EC1M 6BQ, United Kingdom. Tel: +44(0)2078826584;
Or
Dr Li Zhang (li.zhang.uk@googlemail.com), Department of Cardiology, the First Affiliated Hospital, School of Medicine, Zhejiang University, 79 Qingchun Road, Hangzhou, 310003, Zhejiang, China; Tel: +86(0)571-87236500.

Supplementary Figures:

A

Mouse NCKAP1 (NM_016965.3), 3UTR: 3605~4403

Binding site-1 (BS1) - minimum loop-free energy (RNAhybrid):-51.803
3661 ggaactattt taccttaaag cctgaaaaca gttttgtgga tgaaattttc ttcatgctgt
miR-214: 3'-tgacggacagacac----------ggacgaca-5'
BS1^{mut}: taccttaaag cctgaaaaca gttttgtgga tgaaattttc ttAaCgcGTG
Mlu I (ACGGCT)

Binding site-3 (BS3) - minimum loop-free energy (RNAhybrid): -51.80
4141 tccgaggttc tcagacagca gcacatgctg ccgccgcctg tagaaagcct actgtagaaa
miR-214: 3'-tgacggaca-gacacgga cgaca-5'
BS3^{mut}: tgctgccgccgcACgtagaaaCgcGtacACtagaaa
Mlu I (ACGCGT)

Binding site-2 (BS2) - minimum loop-free energy (RNAhybrid): -51.801
4201 catctcatcc cgtgctgccc ggctggcatc tgcactgcct ttac cctgctgtataataaa
miR-214: 3'-tgacg-gacagacac-ggacgaca-5'
BS2^{mut}: ggcatc tAcactgcct ttac AACgcGTGataataaa
Mlu I (ACGCGT)

B

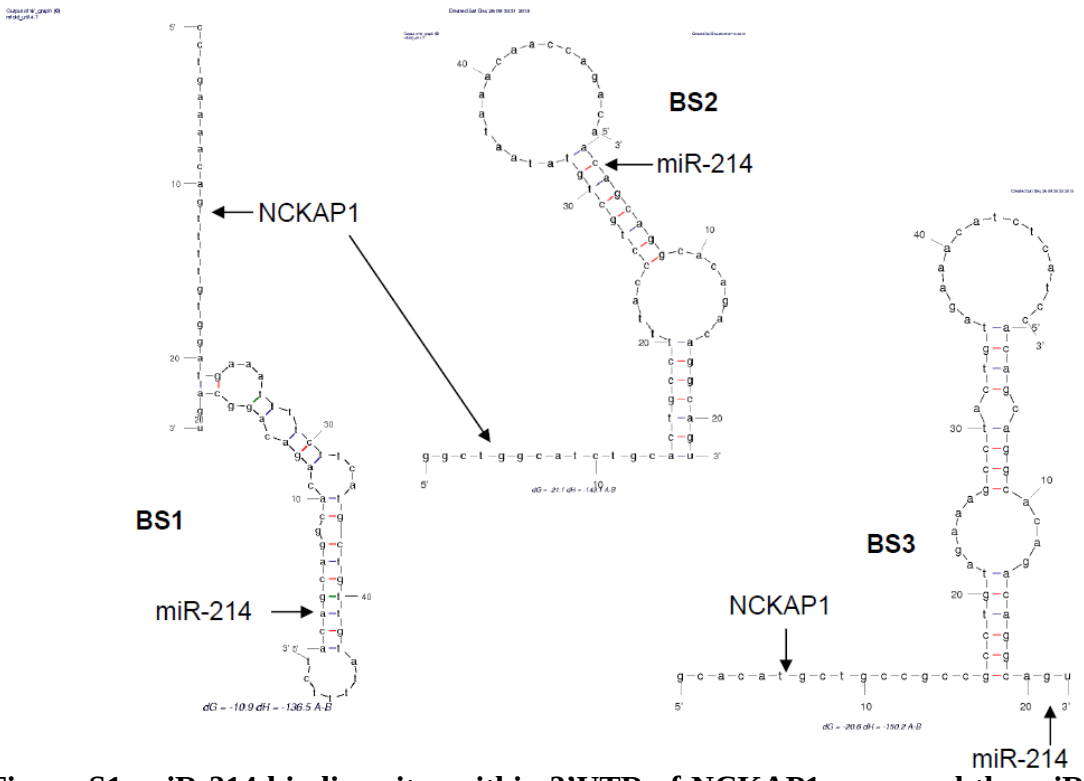

Figure S1. miR-214 binding sites within 3'UTR of NCKAP1 gene, and the miR-214:NCKAP1 3'UTR duplex stem-loop and respective minimum loop-free energy are depicted in this illustration.
(A) Three potential wild type binding sites (BS1-BS3) of miR-214 within NCKAP1 3'UTR as predicted by RNAhybrid and their mutants (BS1/2/3^{mut}) are depicted in this illustration. (B) The formation of the miR-214:NCKAP1 3'UTR (spanning through miR-214 BS1-3) duplex stem-loop and the minimum loop-free energy for individual

loop (binding site) were calculated by and extracted from mFold software (http://mfold.rna.albany.edu/?q=DINAMelt/Two-state-melting).

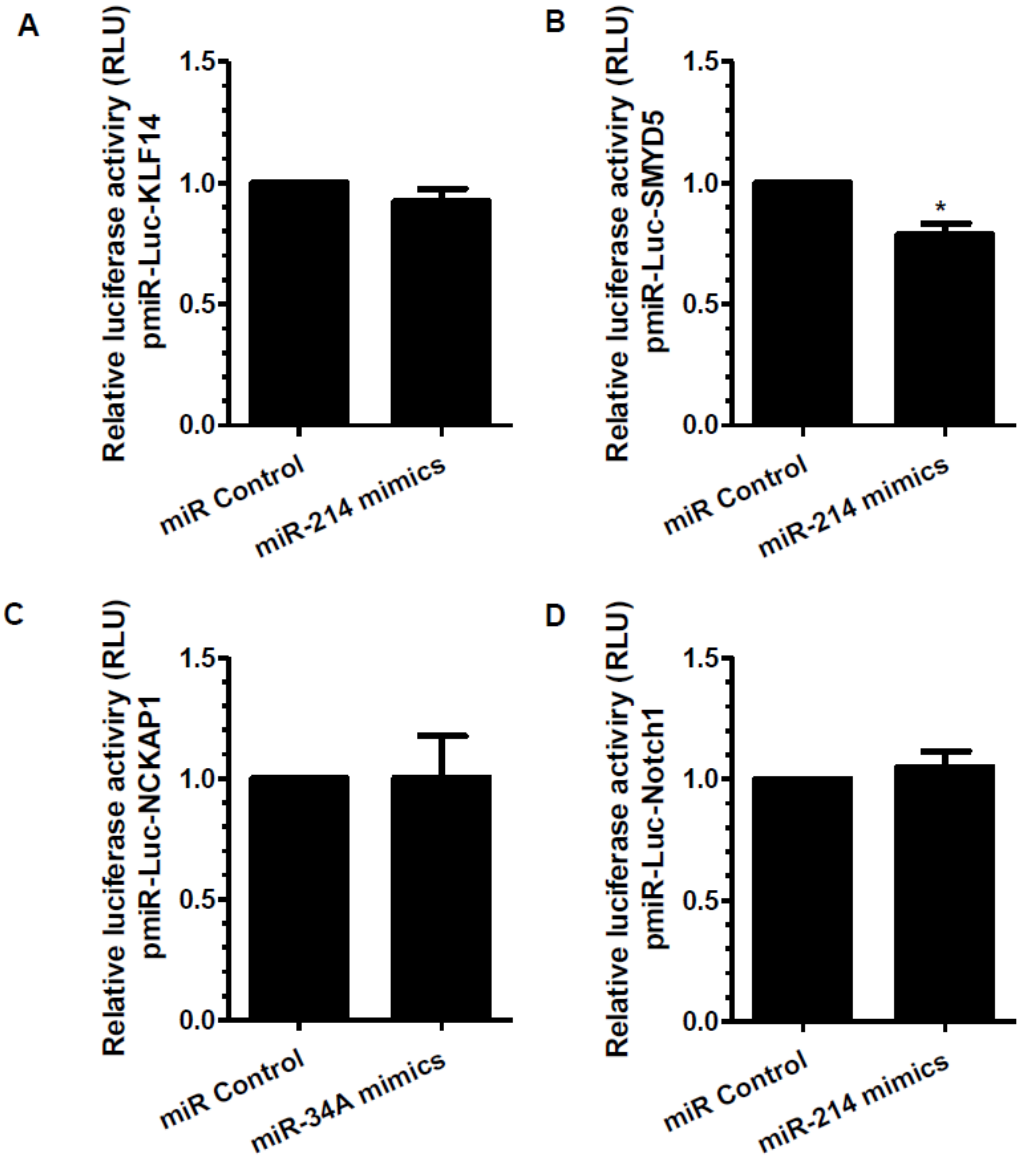

Figure S2. Gene 3'UTR reporter luciferase activity assays.
miR-214 mimics, miR-34A mimics or negative control was co-transfected into VSMCs with respective gene 3'UTR reporter (A, KLF14; B, SMYD5; C, NCKAP1; D, Notch1). Luciferase activity assay were measured at 48 hours post-transfection. The data presented here are representative or mean±S.E.M. of four to six independent experiments (n=4-6). *P<0.05 (versus miR control).

Supplementary table S1: Primer sets used in the present study

Gene names	Forward (5'-3')	Reverse (5'-3')	Application
U6 snoRNA (mu/hu)	GATGACACGCAAATTCGTG	miRNA universal reverse primer (Invitrogen, A11193-051)	Real-time RT-PCR
Mus/hu miR-214 (mature)	CAGGCACAGACAGGCAGT	miRNA universal reverse primer (Invitrogen, A11193-051)	Real-time RT-PCR
Mus Pri-miR-214	GCAAGGCTATGGCACTTACCTA	CCTGTTGTTACTGGCCCTCA	Real-time RT-PCR
Mus NCKAP1	GAGAAGCTCACCATCCTCAAC	CAAGAAGCAAGGACAAGTTTGG	Real-time RT-PCR
Mus PCNA	TTGCACGTATATGCCGAGACCT	ATTGCCAAGCTCTCCACTTGC	Real-time RT-PCR
Mus Twist1	GAGGTCTTGCCAATCAGCCA	CCAGTTTGATCCCAGCGTTT	Real-time RT-PCR
pmiR-Luc-NCKAP1-WT	GTGGTG GAGCTC AGAC AAGCACGAGTTTCTGTTG	CTGCTG AAGCTT CAAGGTGTGATACAGTCTAGTG	NCKAP1 3'UTR reporter clone (Sac I/Hind III)
pmiR-Luc-NCKAP1-BS1^{mu}	gtggatgaaattttcttAaCgcGTgtatttttctgatcattggc	gccaatgatcagaaaataca CACgcGtT aagaaaatttcatccac	miR-214 binding site 1 mutation
pmiR-Luc-NCKAP1-BS2^{mu}	ggcatctAcactgcctttacAACgcGTGataataaacaaccagacac	gtgtctggttgtttattatCACgcGTTgtaaaggcagtgTagatgcc	miR-214 binding site 2 mutation
pmiR-Luc-NCKAP1-BS3^{mu}	tgctgccgccgcACgtagaaCgcGtacACtagaaacatctcatcc	ggatgagatgtttctaGTgtaCgcgttctacGTgcggcggcagca	miR-214 binding site 3 mutation
pmiR-Luc-KLF14	GTCGTC GAGCTC GACTGTCTTGCTGTCTATCT	GTCGTC AAGCTT CTCAGCATTTAAAGATTTATAG	KLF14 3'UTR reporter clone (Sac I/Hind III)
pmiR-Luc-SMYD5	CACGAC GAGCTC TGTTATCTCACCTGGAAGGC	CACGAC AAGCTT TCACCACTCACATTTTATTGAGAC	SMYD5 3'UTR reporter clone (Sac I/Hind III)
pGL3-miR-214-FL	gaggag GAGCTC agggggggagccccaacttatctga	gaggag AAGCTT TTCCTGCACCAGGGGCTTGT	Mouse miR-214 gene promoter (-640:0) clone
pGL3-miR-214-short	gaggag GAGCTC agggggggagccccaacttatctga	ctggtc AAGCTT TGGGGCCCCAGTATGGAAAA	Mouse miR-214 gene promoter (-640:-357) clone

Supplementary table S2: **selected protein list regulated by miR-214 in VSMCs.**

Note: Proteins/genes with yellow-highlighted have been implicated in regulation of cell migration, proliferation, adhesion, actin filament reorganization and actin polymerization, cell cycle, and gene expression, etc.

* Predicted putative target of miR-214 (only the genes with binding sites within 3'UTR have been included in this table)

Proteins	Log FR (Treatment vs Control)	P-value	Fold changes (Treatment vs Control)	Binding sites*	Protein Name
Downregulated proteins by miR-214					
PEPD_MOUSE	-2.737973	0.4	0.149895	No	Xaa-Pro dipeptidase OS=Mus musculus GN=Pepd PE=2 SV=3
ABL2_MOUSE	-1.454600	0.5	0.364856	No	Abelson tyrosine-protein kinase 2 OS=Mus musculus GN=Abl2 PE=1 SV=1
LSM8_MOUSE	-1.454600	0.5	0.364856	No	U6 snRNA-associated Sm-like protein LSm8 OS=Mus musculus GN=Lsm8 PE=3 SV=3
NCKP1_MOUSE	-1.434939	0	0.369863	Yes (3)	Nck-associated protein 1 OS=Mus musculus GN=Nckap1 PE=1 SV=2
HYPK_MOUSE	-1.353127	0	0.391443	yes (1)	Huntingtin-interacting protein K OS=Mus musculus GN=Hypk PE=2 SV=2
COX2_MOUSE	-1.302748	0	0.405353	No	Cytochrome c oxidase subunit 2 OS=Mus musculus GN=Mtco2 PE=1 SV=1
EMAL1_MOUSE	-1.160103	0	0.447481	yes (1)	Echinoderm microtubule-associated protein-like 1 OS=Mus musculus GN=Eml1 PE=1 SV=1
SYAP1_MOUSE	-1.021893	0.5	0.49247	No	Synapse-associated protein 1 OS=Mus musculus GN=Syap1 PE=1 SV=1
SPTB1_MOUSE	-0.918821	0	0.528941	Yes (2)	Spectrin beta chain, erythrocytic OS=Mus musculus GN=Sptb PE=1 SV=4
ILEUC_MOUSE	-0.827446	0.5	0.563526	No	Leukocyte elastase inhibitor C OS=Mus musculus GN=Serpinb1c PE=2 SV=1
LYPA2_MOUSE	-0.806064	0	0.57194	Yes (1)	Acyl-protein thioesterase 2 OS=Mus musculus GN=Lypla2 PE=1 SV=1
KLF14_MOUSE	-0.793026	0	0.577132	Yes (2)	Krueppel-like factor 14 OS=Mus musculus GN=Klf14 PE=2 SV=1
ARPC2_MOUSE	-0.786859	0	0.579604	no	Actin-related protein 2/3 complex subunit 2 OS=Mus musculus GN=Arpc2 PE=1 SV=3
PGM1_MOUSE	-0.786171	0.1	0.579881	No	Phosphoglucomutase-1 OS=Mus musculus GN=Pgm1 PE=1 SV=4
PPM1F_MOUSE	-0.753456	0	0.593181	Yes (3)	Protein phosphatase 1F OS=Mus musculus GN=Ppm1f PE=2 SV=1
ABHEB_MOUSE	-0.704636	0.1	0.613597	No	Alpha/beta hydrolase domain-containing protein 14B OS=Mus musculus GN=Abhd14b PE=2 SV=1
TPP1_MOUSE	-0.689847	0	0.61992	Yes (5)	Tripeptidyl-peptidase 1 OS=Mus

					musculus GN=Tpp1 PE=1 SV=2
SNX12_MOUSE	-0.670723	0.1	0.628192		Sorting nexin-12 OS=Mus musculus GN=Snx12 PE=1 SV=1
CIRBP_MOUSE	-0.659948	0.1	0.632901	No	Cold-inducible RNA-binding protein OS=Mus musculus GN=Cirbp PE=1 SV=1
IDHC_MOUSE	-0.653167	0	0.635883	Yes (2)	Isocitrate dehydrogenase [NADP] cytoplasmic OS=Mus musculus GN=Idh1 PE=1 SV=2
INT3_MOUSE	-0.632013	0	0.645275	Yes (2)	Integrator complex subunit 3 OS=Mus musculus GN=Ints3 PE=2 SV=2
LIMS2_MOUSE	-0.599727	0	0.659879	No	LIM and senescent cell antigen-like-containing domain protein 2 OS=Mus musculus GN=Lims2 PE=1 SV=1
SNX5_MOUSE	-0.595149	0	0.661976	Yes (1)	Sorting nexin-5 OS=Mus musculus GN=Snx5 PE=1 SV=1
SMYD5_MOUSE	-0.572227	0	0.672578	Yes (4)	SET and MYND domain-containing protein 5 OS=Mus musculus GN=Smyd5 PE=2 SV=2
APC7_MOUSE	-0.553523	0	0.681354	Yes (2)	Anaphase-promoting complex subunit 7 OS=Mus musculus GN=Anapc7 PE=1 SV=3
ACOT9_MOUSE	-0.552868	0	0.681664	Yes (2)	Acyl-coenzyme A thioesterase 9, mitochondrial OS=Mus musculus GN=Acot9 PE=1 SV=1
LONM_MOUSE	-0.550077	0	0.682983	Yes (1)	Lon protease homolog, mitochondrial OS=Mus musculus GN=Lonp1 PE=1 SV=2
SNP29_MOUSE	-0.543593	0	0.68606	yes (3)	Synaptosomal-associated protein 29 OS=Mus musculus GN=Snap29 PE=2 SV=1
FKB10_MOUSE	-0.528053	0.4	0.69349	No	Peptidyl-prolyl cis-trans isomerase FKBP10 OS=Mus musculus GN=Fkbp10 PE=1 SV=2
GSTM1_MOUSE	-0.518952	0	0.697878	Yes (2)	Glutathione S-transferase Mu 1 OS=Mus musculus GN=Gstm1 PE=1 SV=2
KIME_MOUSE	-0.515848	0	0.699382	yes (1)	Mevalonate kinase OS=Mus musculus GN=Mvk PE=2 SV=1
ARL3_MOUSE	-0.512953	0	0.700787	Yes (1)	ADP-ribosylation factor-like protein 3 OS=Mus musculus GN=Arl3 PE=1 SV=1
SAMH1_MOUSE	-0.484792	0	0.7146	Yes (2)	Deoxynucleoside triphosphate triphosphohydrolase SAMHD1 OS=Mus musculus GN=Samhd1 PE=1 SV=2
SRRT_MOUSE	-0.483568	0	0.715207	Yes (1)	Serrate RNA effector molecule homolog OS=Mus musculus GN=Srrt PE=1 SV=1
AP2B1_MOUSE	-0.474446	0	0.719743	Yes (6)	AP-2 complex subunit beta OS=Mus musculus GN=Ap2b1 PE=1 SV=1
PROF1_MOUSE	-0.472765	0	0.720582	Yes (2)	Profilin-1 OS=Mus musculus GN=Pfn1 PE=1 SV=2
GSTM2_MOUSE	-0.470258	0	0.721836	Yes (1)	Glutathione S-transferase Mu 2 OS=Mus musculus GN=Gstm2 PE=1 SV=2

CAPZB_MOUSE	-0.463590	0.3	0.725179	No	F-actin-capping protein subunit beta OS=Mus musculus GN=Capzb PE=1 SV=3
TGM2_MOUSE	-0.461355	0	0.726304	Yes (4)	Protein-glutamine gamma-glutamyltransferase 2 OS=Mus musculus GN=Tgm2 PE=1 SV=4
RCN3_MOUSE	-0.457328	0	0.728334	No	Reticulocalbin-3 OS=Mus musculus GN=Rcn3 PE=2 SV=1
SMC3_MOUSE	-0.451019	0	0.731526	Yes (5)	Structural maintenance of chromosomes protein 3 OS=Mus musculus GN=Smc3 PE=1 SV=2
RHOA_MOUSE	-0.447904	0	0.733107	Yes (1)	Transforming protein RhoA OS=Mus musculus GN=Rhoa PE=1 SV=1
G3BP1_MOUSE	-0.444125	0	0.73503	Yes (7)	Ras GTPase-activating protein-binding protein 1 OS=Mus musculus GN=G3bp1 PE=1 SV=1
LAMP1_MOUSE	-0.443885	0	0.735152	Yes (1)	Lysosome-associated membrane glycoprotein 1 OS=Mus musculus GN=Lamp1 PE=1 SV=2
SMC1A_MOUSE	-0.443237	0	0.735483	Yes (1)	Structural maintenance of chromosomes protein 1A OS=Mus musculus GN=Smc1a PE=1 SV=4
SPI2_MOUSE	-0.441805	0.5	0.736213	No	Serpin I2 OS=Mus musculus GN=Serpini2 PE=2 SV=1
PLSI_MOUSE	-0.440962	0	0.736643	Yes (2)	Plastin-1 OS=Mus musculus GN=Pls1 PE=2 SV=1
LTOR3_MOUSE	-0.439528	0	0.737376	Yes (3)	Ragulator complex protein LAMTOR3 OS=Mus musculus GN=Lamtor3 PE=1 SV=1
PSB4_MOUSE	-0.438911	0	0.737691	No	Proteasome subunit beta type-4 OS=Mus musculus GN=Psmb4 PE=1 SV=1
THIM_MOUSE	-0.437870	0	0.738224	Yes (2)	3-ketoacyl-CoA thiolase, mitochondrial OS=Mus musculus GN=Acaa2 PE=1 SV=3
STK25_MOUSE	-0.434782	0	0.739805	Yes (1)	Serine/threonine-protein kinase 25 OS=Mus musculus GN=Stk25 PE=1 SV=2
CATD_MOUSE	-0.434733	0	0.739831	Yes (4)	Cathepsin D OS=Mus musculus GN=Ctsd PE=1 SV=1
ULA1_MOUSE	-0.433753	0	0.740333	No	NEDD8-activating enzyme E1 regulatory subunit OS=Mus musculus GN=Nae1 PE=1 SV=1
TBAL3_MOUSE	-0.433621	0	0.740401	Yes (1)	Tubulin alpha chain-like 3 OS=Mus musculus GN=Tubal3 PE=2 SV=2
CSN5_MOUSE	-0.431786	0.1	0.741343	No	COP9 signalosome complex subunit 5 OS=Mus musculus GN=Cops5 PE=1 SV=3
PPP6_MOUSE	-0.421643	0	0.746574	Yes (2)	Serine/threonine-protein phosphatase 6 catalytic subunit OS=Mus musculus GN=Ppp6c PE=2 SV=1
RS27A_MOUSE	-0.421124	0	0.746842	No	Ubiquitin-40S ribosomal protein S27a OS=Mus musculus GN=Rps27a PE=1 SV=2
CBX1_MOUSE	-0.419343	0	0.747765	Yes (2)	Chromobox protein homolog 1 OS=Mus musculus GN=Cbx1 PE=1 SV=1

MK10_MOUSE	-0.418101	0	0.748409	Yes (3)	Mitogen-activated protein kinase 10 OS=Mus musculus GN=Mapk10 PE=1 SV=2
Upregulated proteins by miR-214					
PSB7_MOUSE	0.323204	0.2	1.251106		Proteasome subunit beta type-7 OS=Mus musculus GN=Psmb7 PE=1 SV=1
DPOE1_MOUSE	0.323513	0.1	1.251374		DNA polymerase epsilon catalytic subunit A OS=Mus musculus GN=Pole PE=2 SV=3
CALX_MOUSE	0.325062	0.3	1.252718		Calnexin OS=Mus musculus GN=Canx PE=1 SV=1
COPZ1_MOUSE	0.326198	0.3	1.253705		Coatomer subunit zeta-1 OS=Mus musculus GN=Copz1 PE=2 SV=1
VPS29_MOUSE	0.327551	0.1	1.254881		Vacuolar protein sorting-associated protein 29 OS=Mus musculus GN=Vps29 PE=1 SV=1
NASP_MOUSE	0.328329	0.1	1.255558		Nuclear autoantigenic sperm protein OS=Mus musculus GN=Nasp PE=1 SV=2
HNRPK_MOUSE	0.328623	0.2	1.255814		Heterogeneous nuclear ribonucleoprotein K OS=Mus musculus GN=Hnrnpk PE=1 SV=1
RTCB_MOUSE	0.328922	0.5	1.256075		tRNA-splicing ligase RtcB homolog OS=Mus musculus GN=Rtcb PE=2 SV=1
UBL4A_MOUSE	0.329965	0.2	1.256983		Ubiquitin-like protein 4A OS=Mus musculus GN=Ubl4a PE=2 SV=1
H12_MOUSE	0.330383	0.3	1.257347		Histone H1.2 OS=Mus musculus GN=Hist1h1c PE=1 SV=2
PHB2_MOUSE	0.332705	0	1.259372		Prohibitin-2 OS=Mus musculus GN=Phb2 PE=1 SV=1
SC61B_MOUSE	0.335326	0.2	1.261662		Protein transport protein Sec61 subunit beta OS=Mus musculus GN=Sec61b PE=1 SV=3
CNPY2_MOUSE	0.339157	0.3	1.265017		Protein canopy homolog 2 OS=Mus musculus GN=Cnpy2 PE=1 SV=1
TRXR1_MOUSE	0.340636	0.1	1.266315		Thioredoxin reductase 1, cytoplasmic OS=Mus musculus GN=Txnrd1 PE=1 SV=3
QCR1_MOUSE	0.341453	0.2	1.267032		Cytochrome b-c1 complex subunit 1, mitochondrial OS=Mus musculus GN=Uqcrc1 PE=1 SV=2
RFA2_MOUSE	0.341865	0	1.267394		Replication protein A 32 kDa subunit OS=Mus musculus GN=Rpa2 PE=1 SV=1
UBE2K_MOUSE	0.343689	0.2	1.268997		Ubiquitin-conjugating enzyme E2 K OS=Mus musculus GN=Ube2k PE=1 SV=3
NUCB2_MOUSE	0.348476	0.3	1.273215		Nucleobindin-2 OS=Mus musculus GN=Nucb2 PE=1 SV=2
ALR_MOUSE	0.349409	0.5	1.274038		FAD-linked sulfhydryl oxidase ALR OS=Mus musculus GN=Gfer PE=2 SV=2
TIA1_MOUSE	0.352377	0.1	1.276662		Nucleolysin TIA-1 OS=Mus musculus GN=Tia1 PE=1 SV=1
TBC15_MOUS	0.353875	0.4	1.277988		TBC1 domain family member 15

E					OS=Mus musculus GN=Tbc1d15 PE=1 SV=1
LSM6_MOUSE	0.356710	0	1.280502		U6 snRNA-associated Sm-like protein LSm6 OS=Mus musculus GN=Lsm6 PE=3 SV=1
IMPA2_MOUSE	0.357044	0.6	1.280799		Inositol monophosphatase 2 OS=Mus musculus GN=Impa2 PE=1 SV=1
VATA_MOUSE	0.360771	0.2	1.284112		V-type proton ATPase catalytic subunit A OS=Mus musculus GN=Atp6v1a PE=1 SV=2
CTBP1_MOUSE	0.364133	0	1.287108		C-terminal-binding protein 1 OS=Mus musculus GN=Ctbp1 PE=1 SV=2
SZT2_MOUSE	0.365471	0.2	1.288303		Protein SZT2 OS=Mus musculus GN=Szt2 PE=1 SV=1
RBM25_MOUSE	0.365489	0	1.288318		RNA-binding protein 25 OS=Mus musculus GN=Rbm25 PE=1 SV=2
PTMS_MOUSE	0.366225	0.7	1.288976		Parathymosin OS=Mus musculus GN=Ptms PE=1 SV=3
INF2_MOUSE	0.367510	0.1	1.290124		Inverted formin-2 OS=Mus musculus GN=Inf2 PE=1 SV=1
ILF3_MOUSE	0.368909	0	1.291376		Interleukin enhancer-binding factor 3 OS=Mus musculus GN=Ilf3 PE=1 SV=2
PABP2_MOUSE	0.371446	0.1	1.293649		Polyadenylate-binding protein 2 OS=Mus musculus GN=Pabpn1 PE=2 SV=3
ALD2_MOUSE	0.372046	0.2	1.294187		Aldose reductase-related protein 2 OS=Mus musculus GN=Akr1b8 PE=1 SV=2
TCOF_MOUSE	0.373927	0	1.295875		Treacle protein OS=Mus musculus GN=Tcof1 PE=1 SV=1
I2BP2_MOUSE	0.374380	0.3	1.296283		Interferon regulatory factor 2-binding protein 2 OS=Mus musculus GN=Irf2bp2 PE=1 SV=1
H32_MOUSE	0.375301	0.2	1.29711		Histone H3.2 OS=Mus musculus GN=Hist1h3b PE=1 SV=2
XRN2_MOUSE	0.376271	0.3	1.297983		5'-3' exoribonuclease 2 OS=Mus musculus GN=Xrn2 PE=1 SV=1
CK5P2_MOUSE	0.376365	0.2	1.298067		CDK5 regulatory subunit-associated protein 2 OS=Mus musculus GN=Cdk5rap2 PE=1 SV=3
RPN1_MOUSE	0.377760	0.1	1.299323		Dolichyl-diphosphooligosaccharide--protein glycosyltransferase subunit 1 OS=Mus musculus GN=Rpn1 PE=1 SV=1
RS28_MOUSE	0.378317	0.3	1.299825		40S ribosomal protein S28 OS=Mus musculus GN=Rps28 PE=2 SV=1
API5_MOUSE	0.378529	0.3	1.300016		Apoptosis inhibitor 5 OS=Mus musculus GN=Api5 PE=1 SV=2
IF2B3_MOUSE	0.379407	0.2	1.300807		Insulin-like growth factor 2 mRNA-binding protein 3 OS=Mus musculus GN=Igf2bp3 PE=1 SV=1
CUL4B_MOUSE	0.379845	0.2	1.301202		Cullin-4B OS=Mus musculus GN=Cul4b PE=1 SV=1
NXT2_MOUSE	0.380032	0.1	1.30137		NTF2-related export protein 2 OS=Mus musculus GN=Nxt2 PE=2

					SV=1
MYL6B_MOUSE	0.382474	0	1.303576		Myosin light chain 6B OS=Mus musculus GN=Myl6b PE=2 SV=1
PYR1_MOUSE	0.384037	0.2	1.304988		CAD protein OS=Mus musculus GN=Cad PE=2 SV=1
RTN4_MOUSE	0.384912	0.1	1.30578		Reticulon-4 OS=Mus musculus GN=Rtn4 PE=1 SV=2
KTN1_MOUSE	0.385735	0.1	1.306525		Kinectin OS=Mus musculus GN=Ktn1 PE=2 SV=1
E2F8_MOUSE	0.386205	0	1.306951		
MALT1_MOUSE	0.386487	0.4	1.307206		Mucosa-associated lymphoid tissue lymphoma translocation protein 1 homolog OS=Mus musculus GN=Malt1 PE=1 SV=2
KLC2_MOUSE	0.388877	0.4	1.309374		Kinesin light chain 2 OS=Mus musculus GN=Klc2 PE=1 SV=1
GFPT2_MOUSE	0.393627	0	1.313692		Glutamine--fructose-6-phosphate aminotransferase [isomerizing] 2 OS=Mus musculus GN=Gfpt2 PE=2 SV=3
BAP31_MOUSE	0.396808	0.1	1.316592		B-cell receptor-associated protein 31 OS=Mus musculus GN=Bcap31 PE=1 SV=4
RAB10_MOUSE	0.405410	0.4	1.324465		Ras-related protein Rab-10 OS=Mus musculus GN=Rab10 PE=1 SV=1
H1T_MOUSE	0.406704	0.2	1.325653		Histone H1t OS=Mus musculus GN=Hist1h1t PE=1 SV=4
NDUA4_MOUSE	0.411036	0.6	1.32964		NADH dehydrogenase [ubiquinone] 1 alpha subcomplex subunit 4 OS=Mus musculus GN=Ndufa4 PE=1 SV=2
RS27L_MOUSE	0.411764	0.2	1.330311		40S ribosomal protein S27-like OS=Mus musculus GN=Rps27l PE=2 SV=3
RRBP1_MOUSE	0.414189	0.2	1.33255		Ribosome-binding protein 1 OS=Mus musculus GN=Rrbp1 PE=1 SV=2
D19L1_MOUSE	0.414387	0.2	1.332733		Probable C-mannosyltransferase DPY19L1 OS=Mus musculus GN=Dpy19l1 PE=2 SV=1
PRUNE_MOUSE	0.414520	0.5	1.332855		Protein prune homolog OS=Mus musculus GN=Prune PE=2 SV=1
UCHL5_MOUSE	0.415921	0.2	1.33415		Ubiquitin carboxyl-terminal hydrolase isozyme L5 OS=Mus musculus GN=Uchl5 PE=1 SV=2
SH3L3_MOUSE	0.420241	0.2	1.338151		SH3 domain-binding glutamic acid-rich-like protein 3 OS=Mus musculus GN=Sh3bgrl3 PE=1 SV=1
AN32B_MOUSE	0.422776	0.4	1.340504		Acidic leucine-rich nuclear phosphoprotein 32 family member B OS=Mus musculus GN=Anp32b PE=1 SV=1
TYB10_MOUSE	0.423131	0.4	1.340834		Thymosin beta-10 OS=Mus musculus GN=Tmsb10 PE=2 SV=3
VASP_MOUSE	0.425311	0.3	1.342862		Vasodilator-stimulated phosphoprotein OS=Mus musculus GN=Vasp PE=1 SV=4
IDHP_MOUSE	0.427113	0.2	1.344541		Isocitrate dehydrogenase [NADP], mitochondrial OS=Mus musculus

					GN=Idh2 PE=1 SV=3
SFR1_MOUSE	0.428830	0.3	1.346141		Swi5-dependent recombination DNA repair protein 1 homolog OS=Mus musculus GN=Sfr1 PE=1 SV=2
CO6A1_MOUSE	0.435420	0.2	1.352304		Collagen alpha-1(VI) chain OS=Mus musculus GN=Col6a1 PE=2 SV=1
CCD38_MOUSE	0.438081	0.4	1.354801		
PPP5_MOUSE	0.439429	0.5	1.356067		Serine/threonine-protein phosphatase 5 OS=Mus musculus GN=Ppp5c PE=1 SV=3
ILF2_MOUSE	0.445389	0.3	1.361681		Interleukin enhancer-binding factor 2 OS=Mus musculus GN=Ilf2 PE=1 SV=1
ERLN2_MOUSE	0.449599	0.1	1.36566		Erlin-2 OS=Mus musculus GN=Erlin2 PE=1 SV=1
TTC9C_MOUSE	0.456300	0	1.372019		Tetratricopeptide repeat protein 9C OS=Mus musculus GN=Ttc9c PE=2 SV=1
SRA1_MOUSE	0.458491	0.1	1.374104		Steroid receptor RNA activator 1 OS=Mus musculus GN=Sra1 PE=1 SV=3
RAB1A_MOUSE	0.461907	0.5	1.377361		Ras-related protein Rab-1A OS=Mus musculus GN=Rab1A PE=1 SV=3
QCR6_MOUSE	0.462570	0.4	1.377995		Cytochrome b-c1 complex subunit 6, mitochondrial OS=Mus musculus GN=Uqcrh PE=1 SV=2
SAE2_MOUSE	0.463759	0	1.379131		SUMO-activating enzyme subunit 2 OS=Mus musculus GN=Uba2 PE=1 SV=1
H2AZ_MOUSE	0.467525	0.2	1.382735		Histone H2A.Z OS=Mus musculus GN=H2afz PE=1 SV=2
SMAD3_MOUSE	0.476613	0.2	1.391473		Mothers against decapentaplegic homolog 3 OS=Mus musculus GN=Smad3 PE=1 SV=2
IKIP_MOUSE	0.477947	0	1.39276		Inhibitor of nuclear factor kappa-B kinase-interacting protein OS=Mus musculus GN=Ikbip PE=2 SV=2
HBA_MOUSE	0.478404	0.4	1.393201		Hemoglobin subunit alpha OS=Mus musculus GN=Hba PE=1 SV=2
CALL3_MOUSE	0.479895	0.5	1.394642		Calmodulin-like protein 3 OS=Mus musculus GN=Calml3 PE=2 SV=1
FBRL_MOUSE	0.481143	0.1	1.395849		rRNA 2'-O-methyltransferase fibrillarin OS=Mus musculus GN=Fbl PE=2 SV=2
ARF4_MOUSE	0.486244	0.2	1.400793		ADP-ribosylation factor 4 OS=Mus musculus GN=Arf4 PE=1 SV=2
GCR_MOUSE	0.488620	0.1	1.403102		Glucocorticoid receptor OS=Mus musculus GN=Nr3c1 PE=1 SV=1
TBCA_MOUSE	0.491108	0.4	1.405524		Tubulin-specific chaperone A OS=Mus musculus GN=Tbca PE=2 SV=3
OFUT2_MOUSE	0.495153	0.4	1.40947		GDP-fucose protein O-fucosyltransferase 2 OS=Mus musculus GN=Pofut2 PE=1 SV=1
LTOR2_MOUSE	0.499423	0.2	1.413648		Ragulator complex protein LAMTOR2 OS=Mus musculus GN=Lamtor2 PE=1 SV=1

ATPD_MOUSE	0.500446	0.3	1.41465		ATP synthase subunit delta, mitochondrial OS=Mus musculus GN=Atp5d PE=1 SV=1
MKLN1_MOUSE	0.500446	0.3	1.41465		
MP2K1_MOUSE	0.501973	0.1	1.416149		Dual specificity mitogen-activated protein kinase kinase 1 OS=Mus musculus GN=Map2k1 PE=1 SV=2
REPS1_MOUSE	0.508337	0.1	1.42241		RalBP1-associated Eps domain-containing protein 1 OS=Mus musculus GN=Reps1 PE=1 SV=2
DHRS4_MOUSE	0.509393	0.2	1.423451		Dehydrogenase/reductase SDR family member 4 OS=Mus musculus GN=Dhrs4 PE=1 SV=3
PTMA_MOUSE	0.525322	0.4	1.439254		Prothymosin alpha OS=Mus musculus GN=Ptma PE=1 SV=2
NC2B_MOUSE	0.527111	0.1	1.441041		Protein Dr1 OS=Mus musculus GN=Dr1 PE=2 SV=1
FETUA_MOUSE	0.530992	0.3	1.444922		Alpha-2-HS-glycoprotein OS=Mus musculus GN=Ahsg PE=1 SV=1
LAP2B_MOUSE	0.531212	0.1	1.445143		Lamina-associated polypeptide 2, isoforms beta/delta/epsilon/gamma OS=Mus musculus GN=Tmpo PE=1 SV=4
PRS10_MOUSE	0.532698	0.4	1.446632		26S protease regulatory subunit 10B OS=Mus musculus GN=Psmc6 PE=1 SV=1
NEST_MOUSE	0.533669	0.2	1.447606		Nestin OS=Mus musculus GN=Nes PE=1 SV=1
NPTN_MOUSE	0.533795	0.1	1.447732		Neuroplastin OS=Mus musculus GN=Nptn PE=1 SV=3
E41L3_MOUSE	0.537226	0.5	1.451179		Band 4.1-like protein 3 OS=Mus musculus GN=Epb41l3 PE=1 SV=1
MEPCE_MOUSE	0.537434	0.2	1.451389		7SK snRNA methylphosphate capping enzyme OS=Mus musculus GN=Mepce PE=1 SV=2
LAP2A_MOUSE	0.537485	0	1.45144		Lamina-associated polypeptide 2, isoforms alpha/zeta OS=Mus musculus GN=Tmpo PE=1 SV=4
SRSF4_MOUSE	0.550978	0	1.465078		Serine/arginine-rich splicing factor 4 OS=Mus musculus GN=Srsf4 PE=2 SV=1
PR40A_MOUSE	0.552884	0	1.467015		Pre-mRNA-processing factor 40 homolog A OS=Mus musculus GN=Prpf40a PE=1 SV=1
H33_MOUSE	0.562486	0.2	1.476811		Histone H3.3 OS=Mus musculus GN=H3f3a PE=1 SV=2
DHRS1_MOUSE	0.567058	0.1	1.481499		Dehydrogenase/reductase SDR family member 1 OS=Mus musculus GN=Dhrs1 PE=2 SV=1
IF1A_MOUSE	0.571096	0	1.485652		Eukaryotic translation initiation factor 1A OS=Mus musculus GN=Eif1a PE=2 SV=3
PP14B_MOUSE	0.595869	0.2	1.511382		Protein phosphatase 1 regulatory subunit 14B OS=Mus musculus GN=Ppp1r14b PE=1 SV=2
IMMT_MOUSE	0.599209	0.1	1.514886		Mitochondrial inner membrane protein OS=Mus musculus GN=Immt

					PE=1 SV=1
MBB1A_MOUSE	0.601030	0	1.5168		Myb-binding protein 1A OS=Mus musculus GN=Mybbp1a PE=1 SV=2
RIR1_MOUSE	0.603171	0	1.519051		Ribonucleoside-diphosphate reductase large subunit OS=Mus musculus GN=Rrm1 PE=1 SV=2
IF2B2_MOUSE	0.607204	0.2	1.523304		Insulin-like growth factor 2 mRNA-binding protein 2 OS=Mus musculus GN=Igf2bp2 PE=1 SV=1
H13_MOUSE	0.627204	0	1.544569		Histone H1.3 OS=Mus musculus GN=Hist1h1d PE=1 SV=2
RANB3_MOUSE	0.630777	0.3	1.548399		Ran-binding protein 3 OS=Mus musculus GN=Ranbp3 PE=1 SV=2
SPF27_MOUSE	0.635218	0.3	1.553173		Pre-mRNA-splicing factor SPF27 OS=Mus musculus GN=Bcas2 PE=2 SV=1
P20L1_MOUSE	0.637010	0	1.555103		PHD finger protein 20-like protein 1 OS=Mus musculus GN=Phf20l1 PE=2 SV=2
HMGA2_MOUSE	0.643604	0.1	1.562227		High mobility group protein HMGI-C OS=Mus musculus GN=Hmga2 PE=1 SV=1
EDF1_MOUSE	0.643840	0.3	1.562482		Endothelial differentiation-related factor 1 OS=Mus musculus GN=Edf1 PE=1 SV=1
TECR_MOUSE	0.644426	0.2	1.563117		Very-long-chain enoyl-CoA reductase OS=Mus musculus GN=Tecr PE=1 SV=1
ITAL_MOUSE	0.649337	0.1	1.568448		Integrin alpha-L OS=Mus musculus GN=Itgal PE=1 SV=2
ABCE1_MOUSE	0.650618	0.1	1.56984		ATP-binding cassette sub-family E member 1 OS=Mus musculus GN=Abce1 PE=2 SV=1
C1QBP_MOUSE	0.665730	0.2	1.586371		Complement component 1 Q subcomponent-binding protein, mitochondrial OS=Mus musculus GN=C1qbp PE=1 SV=1
AT2B2_MOUSE	0.671810	0.2	1.59307		Plasma membrane calcium-transporting ATPase 2 OS=Mus musculus GN=Atp2b2 PE=1 SV=2
DVL3_MOUSE	0.674132	0.3	1.595637		Segment polarity protein dishevelled homolog DVL-3 OS=Mus musculus GN=Dvl3 PE=1 SV=2
RFPLA_MOUSE	0.691521	0.2	1.614985		Ret finger protein-like 4A OS=Mus musculus GN=Rfpl4a PE=2 SV=1
WNK1_MOUSE	0.703097	0.6	1.627996		Serine/threonine-protein kinase WNK1 OS=Mus musculus GN=Wnk1 PE=1 SV=2
NDUS5_MOUSE	0.703673	0.1	1.628646		NADH dehydrogenase [ubiquinone] iron-sulfur protein 5 OS=Mus musculus GN=Ndufs5 PE=1 SV=3
FKB11_MOUSE	0.704716	0.6	1.629824		Peptidyl-prolyl cis-trans isomerase FKBP11 OS=Mus musculus GN=Fkbp11 PE=2 SV=1
SC22B_MOUSE	0.707687	0.1	1.633183		Vesicle-trafficking protein SEC22b OS=Mus musculus GN=Sec22b PE=1 SV=3
PUR8_MOUSE	0.718084	0.1	1.644996		Adenylosuccinate lyase OS=Mus

					musculus GN=Adsl PE=2 SV=2
BIEA_MOUSE	0.734828	0	1.664199		Biliverdin reductase A OS=Mus musculus GN=Blvra PE=2 SV=1
ADT4_MOUSE	0.752110	0	1.684254		ADP/ATP translocase 4 OS=Mus musculus GN=Slc25a31 PE=2 SV=1
H2AY_MOUSE	0.761745	0.3	1.69554		Core histone macro-H2A.1 OS=Mus musculus GN=H2afy PE=1 SV=3
GSLG1_MOUSE	0.771952	0.3	1.707579		Golgi apparatus protein 1 OS=Mus musculus GN=Glg1 PE=1 SV=1
EVL_MOUSE	0.778213	0	1.715005		Ena/VASP-like protein OS=Mus musculus GN=Evl PE=1 SV=2
RPC2_MOUSE	0.780418	0	1.717628		DNA-directed RNA polymerase III subunit RPC2 OS=Mus musculus GN=Polr3b PE=2 SV=2
SLK_MOUSE	0.789592	0.1	1.728586		STE20-like serine/threonine-protein kinase OS=Mus musculus GN=Slk PE=1 SV=2
LARP7_MOUSE	0.790086	0	1.729178		La-related protein 7 OS=Mus musculus GN=Larp7 PE=1 SV=2
ATPG_MOUSE	0.849791	0	1.80224		ATP synthase subunit gamma, mitochondrial OS=Mus musculus GN=Atp5c1 PE=1 SV=1
H2A2B_MOUSE	0.867560	0	1.824574		Histone H2A type 2-B OS=Mus musculus GN=Hist2h2ab PE=1 SV=3
ZBT43_MOUSE	0.883939	0.1	1.845407		Zinc finger and BTB domain-containing protein 43 OS=Mus musculus GN=Zbtb43 PE=2 SV=2
HECD1_MOUSE	0.898640	0.3	1.864307		E3 ubiquitin-protein ligase HECTD1 OS=Mus musculus GN=Hectd1 PE=1 SV=2
ALBU_MOUSE	0.907684	0.3	1.876031		Serum albumin OS=Mus musculus GN=Alb PE=1 SV=3
MEP50_MOUSE	0.921289	0.4	1.893807		Methylosome protein 50 OS=Mus musculus GN=Wdr77 PE=1 SV=1
MAP6_MOUSE	0.960701	0	1.946255		Microtubule-associated protein 6 OS=Mus musculus GN=Map6 PE=1 SV=2
PLP2_MOUSE	0.968741	0.4	1.957132		Proteolipid protein 2 OS=Mus musculus GN=Plp2 PE=2 SV=1
M4K4_MOUSE	1.004881	0.1	2.006777		Mitogen-activated protein kinase kinase kinase kinase 4 OS=Mus musculus GN=Map4k4 PE=1 SV=1
EHD3_MOUSE	1.008355	0	2.011615		EH domain-containing protein 3 OS=Mus musculus GN=Ehd3 PE=1 SV=2
FBLN3_MOUSE	1.010373	0.1	2.014431		EGF-containing fibulin-like extracellular matrix protein 1 OS=Mus musculus GN=Efemp1 PE=2 SV=1
PI3R4_MOUSE	1.022615	0.2	2.031597		Phosphoinositide 3-kinase regulatory subunit 4 OS=Mus musculus GN=Pik3r4 PE=1 SV=3
HAP28_MOUSE	1.123091	0.7	2.178132		28 kDa heat- and acid-stable phosphoprotein OS=Mus musculus GN=Pdap1 PE=1 SV=1
ATPO_MOUSE	1.164437	0.6	2.241457		ATP synthase subunit O, mitochondrial OS=Mus musculus

					GN=Atp5o PE=1 SV=1
NUFP2_MOUSE	1.298795	0.1	2.460232		Nuclear fragile X mental retardation-interacting protein 2 OS=Mus musculus GN=Nufip2 PE=1 SV=1
MRCKB_MOUSE	1.353744	0.3	2.555745		Serine/threonine-protein kinase MRCK beta OS=Mus musculus GN=Cdc42bpb PE=1 SV=2
CPPED_MOUSE	1.474910	0	2.779663		Serine/threonine-protein phosphatase CPPED1 OS=Mus musculus GN=Cpped1 PE=2 SV=1
ABRA_MOUSE	1.561250	0.3	2.951095		
H2AX_MOUSE	1.567391	0.1	2.963682		Histone H2AX OS=Mus musculus GN=H2afx PE=1 SV=2
BRCC3_MOUSE	1.613716	0.4	3.060391		Lys-63-specific deubiquitinase BRCC36 OS=Mus musculus GN=Brcc3 PE=2 SV=1
ARP3B_MOUSE	1.795556	0.6	3.471492		Actin-related protein 3B OS=Mus musculus GN=Actr3b PE=2 SV=1
FRIL2_MOUSE	2.195888	0.4	4.581715		Ferritin light chain 2 OS=Mus musculus GN=Ftl2 PE=2 SV=2
Other reported targets of miR-214					
CTNB1_MOUSE	-0.181716	0.6	0.881654		Catenin beta-1 OS=Mus musculus GN=Ctnnb1 PE=1 SV=1
PCBP2_MOUSE	-0.042262	0.8	0.971131		Poly(rC)-binding protein 2 OS=Mus musculus GN=Pcbp2 PE=1 SV=1

Supplementary table S3: **GO term enrichment analysis of down-regulated proteins by miR-214 in VSMCs.**

Analysis Type:	PANTHER Overrepresentation Test (release 20160321)						
Annotation Version and Release Date:	GO Ontology database Released 2016-04-23						
Analyzed List:	Down-regulated (Mus musculus)						
Reference List:	Mus musculus (all genes in database)						
Bonferroni correction:	TRUE						
GO biological process complete	**Mus musculus - REFLIST (22320)**	**Proteins (56)**	**Proteins (expected)**	**Proteins (over/under)**	**Proteins (fold Enrichment)**	**Proteins (P-value)***	**Protein name**
regulation of actin filament polymerization (GO:0030833)	137	6	0.34	+	17.46	1.05E-02	NCKPA1, RHOA, ARPC2, SPTB1, PROF1, CAPZB
regulation of protein polymerization (GO:0032271)	174	7	0.44	+	16.03	2.29E-03	NCKPA1, RHOA, ARPC2, SPTB1, PROF1, CAPZB, EMAL1
regulation of actin polymerization or depolymerization (GO:0008064)	156	6	0.39	+	15.33	2.21E-02	NCKPA1, RHOA, ARPC2, SPTB1, PROF1, CAPZB
regulation of actin filament length (GO:0030832)	157	6	0.39	+	15.23	2.30E-02	NCKPA1, RHOA, ARPC2, SPTB1, PROF1, CAPZB
regulation of actin cytoskeleton organization (GO:0032956)	278	7	0.7	+	10.04	4.99E-02	NCKPA1, RHOA, ARPC2, SPTB1, PROF1, CAPZB, PPM1F
organelle organization (GO:0006996)	2779	21	6.97	+	3.01	1.30E-02	NCKAP1, RHOA, STK25, SNX12, PLSI, THIM, TPP1, CATD, EMAL1, ARPC2, PPM1F, PROF1, ABL2, SMC3, ARL3, SNX5, SNP29, LONM, SMC1A, CAPZB, APC7